

**Effect of Hexa Boron Nitride and REO addition on wear and
corrosion behavior of hard-facing on mild steel**

A Dissertation submitted

in partial fulfilment of requirements
for the degree of

Master of Engineering

in

Production Engineering

by

Sikander^{Pal} Singh

Registration No.: 801685017

Under the supervision of

Dr.R.S. Joshi (Supervisor)

(Assistant Professor, MED)

Dr. V.K. Singla (Supervisor)

(Associate Professor, MED)



THAPAR INSTITUTE
OF ENGINEERING & TECHNOLOGY
(Deemed to be University)

MECHANICAL ENGINEERING DEPARTMENT

TIET, PATIALA

JULY, 2018

CERTIFICATE

I hereby declare that this thesis report entitled "Effect of Hexa Boron Nitride and REO addition on wear and corrosion behavior of hard-facing on mild steel" is an authentic record of my work carried out as requirements for the award of the degree of Master of Engineering in Production Engineering at Thapar Institute of Engineering & Technology, Patiala under the supervision of Dr. R. S. Joshi (Assistant Professor, MED) and Dr. V.K. Singla (Associate Professor) No part of the matter embodied in this report has been submitted to any other university or institute for the award of any degree.

31/07/2018
Date:

Sikander Pal Singh
Sikander Pal Singh
801685017
TIET, Patiala

It is certified that the above statement made by the student is correct to the best of our knowledge and belief.

Dr. R. S. Joshi
Assistant Professor, MED
TIET, Patiala - 147004

Dr. V.K. Singla
Associate Professor, MED
TIET, Patiala - 147004

ACKNOWLEDGEMENTS

I would like to express my deep gratitude towards my supervisors, Dr. R.S. Joshi and Dr. Vinod Kumar Singla, Department of Mechanical Engineering, Thapar Institute of Engineering and Technology, Patiala for their valuable guidance and support. Working under their guidance has been fruitful and worthwhile in the context of knowledge. I also like to thank Dr Sukwinder Panesar, Assistant Manager and Head, Alpha Test House at Mohali and all the other staff members as well for providing facilities for experimentation. I would also like to thank all the lab attendants at Thapar Institute of Engineering and Technology, Patiala for their valuable support in carrying out experimentation on SEM, wear testing, Microhardness testing.

I am very thankful to my parents, friends and colleagues for their support in preparation of this thesis report.



Sikander pal Singh

801685017

TIET, Patiala

ABSTRACT

Hard-facing technique improves the mechanical properties of material as well as chemical properties also. It increases the service life of metal. Use of hard-facing in many wide applications like concrete mixer, rock crusher, crane jaws, sugarcane rollers etc. This technique improves the wear resistant and corrosion resistant of material. It improves the hardness also. This study was revealed the effect of hexa boron nitride and lanthanum oxide additive on wear resistance and corrosion resistance of hard-facing on mild steel of grade E-250, which was developed by an manual arc welding process. Wear test performed by pin-on-disc machine. Microstructure and size of grains were studied by EBSD (Electron backscatter diffraction). Corrosion test was performed by salt spray chamber. Experiment duration in salt spray chamber was 120 hours. Hardness of the element on hard-facing layer was measured by vickerhardness test. Four samples were prepared sample N (addition of HBN), sample A (addition of no element), sample LN (addition of lanthanum oxide and HBN) and sample L (addition of lanthanum oxide). The results were shown that with addition of hexa boron nitride hardness of weld layer was enhanced and with addition of lanthanum hardness was decreased. Hardness in case of HBN expanded by 20 % but lanthanum reduced the hardness by 2 % as compared to sample A. Combination of HBN and lanthanum oxide enhanced the hardness by 14.5 % as compared to that sample in which no element was added. Grain size with addition of hexa boron nitride reduced to 3.78214 ± 1.22594 microns. Lanthanum oxide increased the size of grains to 17.825 ± 2.5877 microns. Grains size of reference sample A in which no element was added was 10.5847 ± 2.59363 microns. In combination of both the HBN and La_2O_3 reduced the grains size which was 5.63378 ± 1.55312 microns. In corrosion experiment, addition of HBN increased the corrosion rate. 60% area of the weld bead of sample got corrosion in which HBN was added. HBN reduced the corrosion resistance. Lanthanum oxide enhanced the corrosion resistance. Only 15 % area of weld bead was corroded of sample L in La_2O_3 was added. In the combination of both HBN and lanthanum oxide 15 % area of weld bead corroded. Wear resistance of HBN was good as compared to reference sample A. Lanthanum oxide and HBN were shown good wear resistance than reference sample A because of less weight loss. Sample A got 0.014 g weight loss at 49.05 N load and 6000 m sliding distance. Sample N got 0.011g weight loss at 49.05 N load and 4200 m sliding distance. Sample LN got same weight loss as sample N at same loading condition and same sliding distance.

CONTENTS

S. NO	TITLE	PAGE NO
	Candidates Certificate	I
	Acknowledgement	II
	Abstract	III
	List of Tables	VI
	List of Figures	VII
	Nomenclature	IX
1	CHAPTER 1 INTRODUCTION	1-8
	1.1.1 Build-up	1
	1.1.2 Weld cladding	1
	1.1.3 Buttering	1
	1.1.4 Hard-facing	1
	1.2.1 RE-BUILDING	1
	1.2.2 Buffer Layer	2
	1.3.1 Low Impact	33
	1.3.2 High stress abrasion	3
	1.3.3 High Impact	3
	1.3.4 Adhesion/high friction	3
	1.3.5 Erosion	3
	1.3.6 Cavitation	3
	1.3.7 Thermal fatigue	3
	1.3.8 Fretting	3
	1.4 Corrosion	4
	1.4.1 Types of corrosion	4
	1.5 Benefits of hard-facing	4-5
	1.6 Weld bead patterns	5
	1.7.1 Arc welding	6
	1.7.2 Shielded metal arc welding	6
	1.7.3 Submerged arc welding	6
	1.7.4 Plasma arc welding	7
	1.7.5 Tungsten inert gas welding	7
	1.7.6 Metal inert gas welding	7
	1.7.7 Electroslag welding	7
	1.7.8 Resistance spot welding	8

2	CHAPTER 2 LITERATURE REVIEW	9-16
3	CHAPTER 3 PROBLEM FORMULATION	17
4	CHAPTER 4 METHODOLOGY	18-28
	4.1 INTRODUCTION	18
	4.3 Material used as base metal	18
	4.4 Prepared the specimen for welding	19
	4.5 Manual arc welding set	19
	4.6 Welding parameter	20
	4.7 Welding Electrode	20
	4.8 Preparation of manual arc welding process	21
	4.9 Powder used as ingredients	22
	4.10.1 Micro hardness Test	23
	4.11 Disk Polisher Machine	24
	4.12 EBSD (Electron Back Scattered Diffraction)	24-25
	4.13 Salt spray chamber for corrosion test	25-26
	4.14 SEM (Scanning Electron Microscope)	26
	4.15 Wear test performed on pin-on-disc machine	27
	4.15.1 Material used for disc	27
	4.15.2 Weigh Machine	27
	4.15.3 Pin-on-Disc Experiment	28
5	CHAPTER 5 RESULTS AND DISCUSSION	29-53
	5.1 Electron backscatter diffraction	29-37
	5.2.1 Micro hardness Test	37-39
	5.3 Wear test analysis	39
	5.3.1 Results of wear test was performed at 49.05 N load and 2 m/s speed	40-42
	5.3.2 Results of wear test Performed at 73.575 N load and speed 2 m/s	43-46
	5.3.3 SEM Images of wear samples	47
	5.4 Results for corrosion test of weld bead	48-51
	5.4.5 SEM Images of corrosion samples	51-53
6	CHAPTER 6 CONCLUSIONS	54-55
7	REFERENCES	56-58

LIST OF FIGURES

S. NO.	TITLE	PAGE NO.
1	Figure 1.1 Buffer layer and Rebuilding Layer	2
	Figure 1.2 Types of corrosion	4
	Figure.1.3 Types of pattern of weld bead	5
	Figure 4.1 Steel Plates with groove	19
	Figure 4.2 Manual arc Welding Setup	20
	Figure 4.3 Electrodes used for hard-facing	21
	Figure 4.4 groove filled with powder	21
	Figure 4.5 Weld bead	22
	Figure 4.6 Micro hardness testing machine	23
	Figure 4.7 Surface grinder	23
	Figure 4.9 Disk polisher	24
	Figure 4.10 Sample after polishing	24
	Figure 4.10 Electropolishing machine	25
	Figure 4.11 Samples after electropolishing	25
	Figure 4.12 Salt Spray Chamber	26
	Figure 4.13 SEM machine	26
	Figure 4.14 Samples for wear	27
	Figure 4.15 Disk of EN 31 steel grade	27
	Figure 4.16 Weigh machine	28
	Figure 4.17 Pin on disc machine	28
	Figure 5.1 EBSD map and inverse pole figure of sample A (Reference)	29
	Figure 5.2 EBSD map and inverse pole figure of sample N	30
	Figure 5.3 EBSD map and inverse pole figure of sample LN	30
	Figure 5.4 EBSD map and inverse pole figure of sample L	31
	Figure 5.5 (a) EBSD map of grain size distribution with area fraction (b) Grain misorientation distribution on the top surface of weld bead of sample A	31-32
	Figure 5.6 (a) EBSD map of grain size distribution with area fraction (b) Grain misorientation distribution on the top surface of weld bead of sample N	32-33

Figure 5.7	(a) EBSD map of grain size distribution with area fraction (b) Grain misorientation distribution on the top surface of weld bead of sample LN	33-34
Figure 5.8	(a) EBSD map of grain size distribution with area fraction (b) Grain misorientation distribution on top surface of weld bead of sample L	34-35
Figure 5.9	Bar graph show hardness (VHN) of hard-facing deposition of different element	38
Figure 5.10	Graph plots of weight loss and sliding distance at load 49.05 N sample A	40
Figure 5.11	Graph plots of weight loss and sliding distance load 49.05 N sample N	41
Figure 5.12	Graph plots of weight loss and sliding distance load 49.05 N sample LN	42
Figure 5.13	Graph plots of weight loss and sliding distance at load 73.575 N sample A	43
Figure 5.14	Graph plots of weight loss and sliding distance at load 73.575 N sample N	44
Figure 5.15	Graph plots for weight loss and sliding distance at load 73.575 N sample LN	45
Figure 5.16	SEM images of surface of weld bead of wear sample (a) Sample N (b) Sample A (c) Sample LN	47
Figure 5.17	Corrosion of weld bead of sample A from 0 hours to 120 hours	48
Figure 5.18	Corrosion of weld of sample N from 0 hour to 120 hours	49
Figure 5.19	Corrosion of weld bead of sample L form 0 hour to 120 hours	50
Figure 5.20	Corrosion of weld bead of sample LN from 0 hour to 120 hours	50
Figure 5.21	Corrosion %age of area of weld bead of each sample	51
Figure 5.22	SEM images of surface morphology of corrode weld bead (a) Sample A (b) Sample N (c) Sample L (d) Sample LN	51-52

NOMENCLATURE

HBN	Hexa Boron Nitride
La ₂ O ₃	Lanthanum oxide
m/s	meter/second
VHN	Vicker hardness number
Wt%	weight percentage
mg	milligram
µm	micrometer
N	Newton
m	metre
Rpm	Radius per minute
wtd	Wear track diameter
mm	millimeter
V	Voltage
A	Ampere
ASTM-B-117-11	Standard for salt spray chamber
EBSD	Electron backscattered diffraction
SEM	Scanning electron microscope
XRD	X-ray diffraction
EN 31steel	Emergency number 31steel
E-250	Engineering steel

CHAPTER 1

INTRODUCTION

Surfacing is a sophisticated technique to improve the wear and corrosion resistance as well as strength of the metal. This technology is widely used in industries for many purposes. It increases the life of component or tool by augmentation the strength. Surfacing can alter the properties of surface of metal to enhance the wear resistance and corrosion resistance[19].

1.1 Surfacing can be done by four methods

1.1.1 Build-up This process is used to recover the dimensions of that parts of machine tool, which are worn during manufacturing for example: size of machine tool get reduces after induction of wear then Welding should be done to recover the size of worn part of machine tool [19].

1.1.2 Weld cladding In many applications like fossil fuel power plants and gating system over dams etc. there is risk of corrosion. To prevent metal from corrosion, weld overlay or cladding is used by providing filler material to base metal[19].

1.1.3 Buttering This process is used to joining of two base metal of different metal by addition of filler material with help of welding technique. It eradicate the effect of PWHT (post weld heat treatment)[19].

1.1.4 Hard-facing This process is used to avoid defects like soundness and improve the toughness of material to resist the impact. Put a stop to environmental condition (corrosion and from hot gaseous). It enhances the wear resistance of material and improves the hardness of the surface of metal [19].

1.2 Hard-facing Terminologies

1.2.1 Re-Building It is refurbishment of machine tool to its initial dimensions, which tool has been worn out with excess use during production. It is deposition of weld layer on base metal and after deposition, grinds the weld layer to make the flat surface of tool or to get rid of discontinuity of distribution of filler material. Mechanical and chemical properties of rebuilding layer are similar to those of base metal or In some cases it is heterogeneous [20].

1.2.2 Buffer Layer This is layer of welding, over the re-building layer to support the hard-facing layer. After welding, there are many types of failure occur like shrinkage of weld bead and cracks etc. To overcome these problems, buffer layers deposits on base metal. After immediate cooling of weld bead, cracks and stresses induced which may be reason of failure of the product. So, buffer Layer is high quality base for hard-facing layer [20].

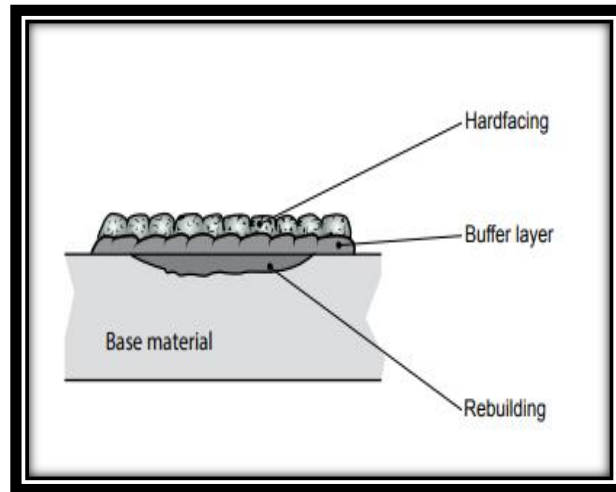


Figure 1.1 Buffer layer and Rebuilding Layer [20]

1.3 Types of wear which affects the base metals

Wear is defined as removal of material with excess use or it occurs when metal to metal surface has relative frictional motion. It reduces the life and deteriorates the surface of part. It raises significant cost of the part. Increases the loss of power (Teeth of the gears are worn with friction and reduces the power transmission in automobiles). Wear destroys the mechanical properties of part like yield, elasticity, toughness and strength etc. To overcome this problem in low cost and to get optimum performance for more life time, hard-facing should be done on part. It increases the life of part more than 300 times [3]. Geometry is very important factor for base metal. It informs us which type of wear will occur and which type of welding is required for repair (rebuilding or hard-facing). Factors which affects the design of parts for example:-Motions like velocity, rotation, oscillations and at which angle, pressure will apply, how much these factor damage the part. Environmental conditions like humidity, temperature and pressure etc. it is very important to choose the environmental factor for welding [20].

1.3.1 Low Impact Wear particles are slide on other surface and apply very low pressure. It can never change the dimension of the surface. Mostly use of this technique in micromachining to remove the material [20].

1.3.2 High stress abrasion In this type of wear, when high pressure will apply on abrasive particle and deteriorate the particles into many pieces. Due to high pressure, chips are formed. For example: Rock crushers [20].

1.3.3 High Impact This type of wear induces due to high impact of load, which produces the discontinuous chips and scratches. To beat this problem ductile material is used. In Rock crusher application it has been found[20].

1.3.4 Adhesion/high friction This type of wear occurs when two bodies rub against each other and under high pressure or high temperature material of on body sticks to other body. Factor affecting in this type of wear are friction coefficient, relative speed and high temperature etc. this defect cannot be seen by naked eyes[20].

1.3.5 Erosion Erosion is occur by strikes the abrasive particle with liquid at high velocity. It depends on angle of striking of the abrasive particle and liquid or speed of striking of jet. Erosion depends on hardness of substrate i.e how much material will remove. Chips are produced or abrasive particle get distorted in shape when they strikes the surface of the metal at higher angle. So it is necessary to choose the metal, which absorb the energy at higher rate[20]

1.3.6 Cavitation Cavitation occurs due to high impact of jet of liquid. It mostly occurs in turbine blade. Formation of cavities takes place, where jet strikes the liquid on blade. Material of high toughness should be used to resist the cavitation [20].

1.3.7 Thermal fatigue This type of wear occur where thermal cycle repeated and base metal cooled and heated after every repeated cycle of load .Due to quickly change of temperature of base metal surface cracks occur .it is known as “thermal fatigue loading”. For example: Hot rollers, forge tool etc[20].

1.3.8 Fretting It is type of wear in which continuous removal of material, when there is sliding or rolling motion between two bodies. Wear occur in the form of chipping and pitting[20].

1.4 Corrosion

It is very complex challenge to get rid of corrosion .material become scrap if it gets corrosion. Major factor for corrosion is environmental condition. corrosion occur due to geometry of part if there is uniformities metal structure or if there is hole in metal. Oxidation occurs when protective layer of oxide film will damage. Corrosion is not a major issue when hard-facing is done [21]

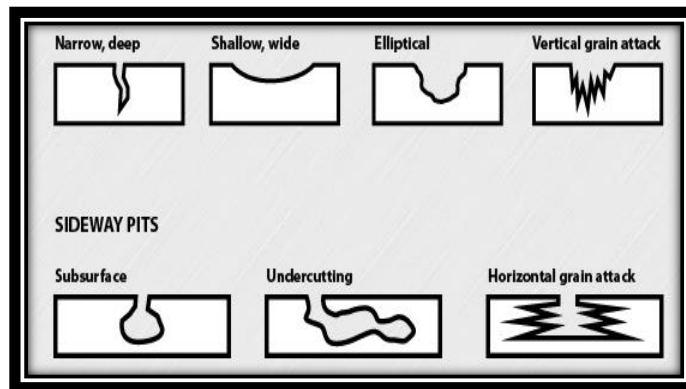


Figure 1.2 Types of corrosion [21]

1.4.1 Types of corrosion

1.4.1.1 Pitting corrosion It produces cavities and deteriorates the metal. Metal will loss its weight due to depassivation. Pitting corrosion assaults regularly occurs at focuses where the passive layer may be debilitated, for instance by slag considerations, a harmed surface or blemishes in the passive layer. Once the assault has begun, the material can be totally damaged in short time[21].

1.4.1.2 Crevice corrosion This corrosion occurs in very narrow spaces. Mechanism of corrosion is same as pitting corrosion[21].

1.4.1.3 Intergranule corrosion This type of corrosion directly attack on the grain boundary. It occurs due to depletion of layer of chromium carbide.

1.4.1.4 Galvanic corrosion This corrosion occurs, when two dissimilar materials connect by welding or by other method. Two different materials produce corrosion potential due to difference in electrical conductivity [21].

1.5 Benefits of hard-facing

1. It reduces the time for repair
2. It reduces the cost for maintenance
3. It increases the service life of old tool
4. It improves the mechanical properties of metal

5. It increases the toughness
6. It improves the corrosion resistant of metal
7. It recovers the size of worn part of machine tool

1.6 Weld bead patterns

Weld bead pattern provides good wear resistance than simple bead pattern in hard-facing. Select the pattern for weld bead, according to type of applications [20].

1.6.1 Various type of pattern

1. Juxtaposed passes
2. Regular interval
3. Grid passes
4. Spot weld

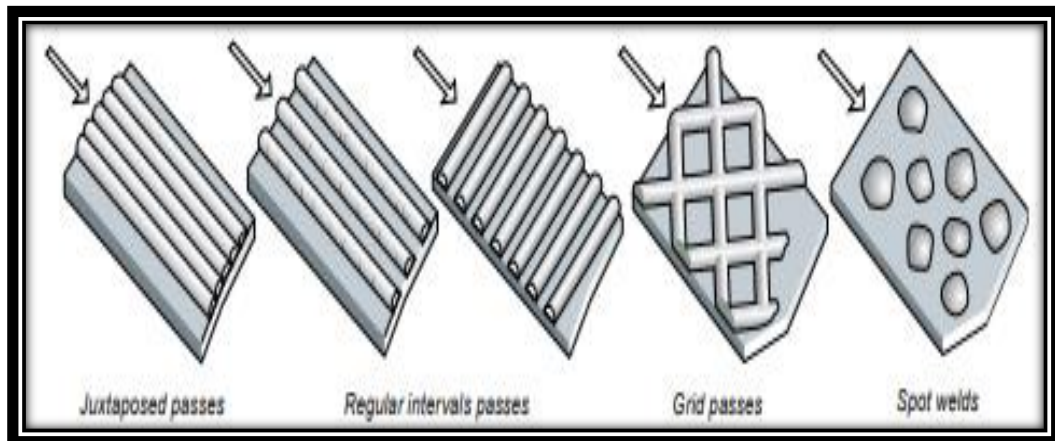


Figure.1.3 Types of pattern of weld bead [20]

Juxtaposed passes type of pattern becomes the barrier between external element and base metal. Complete surface of base metal covers with weld beads. There is no space or gap between two weld beads. In Regular interval passes, weld beads are deposited at small distance from each others. Main purpose of this pattern is that to prevent the base metal from high abrasion. Small spaces between the beads prevent the contact of the surface of base metal with larger abrasion. In grid passes pattern, weld beads are deposited in cross pattern. Beads make 30° angle or 90° angle with each other. Small abrasive gets stuck in beads and prevent the surface of base metal from large abrasives. Spot weld pattern, designed for those steel which are less sensitive for high temperature. The purpose of the dotted type pattern is to reduce the welding stresses [20]

1.7 Types of hard-facing processes

1.7.1 Arc welding Heat required for the melting of plate is obtained due to electric arc, it is called an electric arc. When power supply transfer and optimum gap maintains between tip of electrode and workpiece, the high velocity electron will be generated at the cathode, which are attracted by anode and move towards anode. When electron impinges on the anode, the kinetic energy of electron will be converted into heat energy. The heat generates at the anode, simultaneously the high velocity positively charged ions generates at anode which attracts by cathode and move towards cathode. When high velocity ions impinges on cathode, the K.E of ions converts into heat energy and heat generate at cathode also but velocity of electrons is much higher than ions. Heat generates at anode is higher than cathode. During this process, some of the negatively charged electrodes and positively charged ions will collide in the passage, so that K.E of both the elements will be spontaneously converted into heat energy, which is observed as spark between anode and cathode. Due to this sparking, the temperature induces in the arc in range of 5000 °C to 6000 °C. In this zone ultraviolet rays are generate and spreads around the arc.

1.7.2 Shielded metal arc welding SMAW works on same principle of arc welding process, that why it is arc welding process. Consumable electrode uses for SMAW process. Electrode coated with flux which provides shielding to surface of metal. Heat produces after the arc generates and this heat melts the fluxes which provide alloys to bead material. Bead becomes harder than even the base metal. SMAW current remains in the range of 30 to 300 A. Voltage varies from 15 to 45 V.

1.7.3 Submerged arc welding In this the arc is completely submerged in the flux powder. Continuously consumable electrode wound on spool and fed by action of gravity. Large quantity of flux powder will supplied through the hopper, out of which some amount of flux powder is melting and converting into the slag-remaining flux powder is simply floating on the top that is unused flux. It collects and reuse by hopper. Size of the weld pool powder as compare to arc is larger. Welding of large thickness plates is done in a single pass. Due to the force of arc, the molten metal particles are trying to jump from weld pool but presence of large quantity of flux over weld pool restricts the jumping of molten metal particles. It reduces the spatter.

1.7.4 Plasma arc welding In this process plasma gas turned into plasma by absorb the energy from spark. Spark initiated between tungsten electrode and metal surface. Plasma stands for 50000° C temperature but welding is done over 20000°C temperature only. High temperature is uses collect the electrons to produce atom and then gases produce which releases the heat and melt the metal surface

1.7.5 Tungsten inert gas welding The tungsten is used as electrode material and considered as non consumable electrode. To protect the weld pool from atmospheric contamination, the inert gas would be supplied to the welding pool continuously using inert gas cylinder. The most commonly used inert gas is argon. To avoid the melting of electrode, coolant will be applied, through a small pipe, which is wrapped around the electrode. So, that the temperature of electrode is kept as low as possible.

1.7.6 Metal inert gas welding It uses consumable electrode, which requires no need to supply any coolant. Hence cost of welding reduces. Due to consumable electrode, it is possible to join more than 5 mm thickness rod without using any additional filler material. When electrode touches the rubber pad, any air particles sticking to the surface can be squeezed out because electrode itself is consumable, no tungsten diffusion. Maximum size of electrode would be 3-4 mm. During joining of large thickness plates in single pass with mig welding, speed of welding must be low because of small size of electrode. Size of weld pool as compare to arc is very large. Due to the force of arc, molten particles easily jump from weld pool and spatter loss would become very high.

1.7.7 Electroslag welding It is a special welding process, which can be used for joining plates of above 75 mm in single pass. It is only used in vertical welding position. When power supply is on, arc produces between tip of electrode and workpiece. The heat generated due to the arc can be used only for melting of the electrically conducting flux powder and forming as molten slag, so that tip of electrode will be immersed inside the molten slag and arc is put off. Now electricity is flowing from electrode to workpiece through electrical conductivity of molten slag. When current is passing through molten slag, because of electrical resistance of the slag, the heat is getting generated and heat will be used for melting of the plates and electrodes. Heat required for melting of plates is obtained due electrical resistance of molten slag.

1.7.8 Resistance spot welding The heat required for melting of plates and joining is produced because of electrical resistance. That is why It is called resistance welding. The shape of weld bead produced is approximately like spark called as spark welding. It is fusion pressure welding process. Non consumable electrode material should have low electrical resistance, high melting point and higher strength.

CHAPTER 2

LITERATURE REVIEW

Keeping in mind the end goal to recognize the destinations of present examination, an extensive writing survey was led. An endeavor was made to survey the writing on effect of welding layer on different types of metals like stainless steel, mild steel, grey cast iron etc. to improve the mechanical properties of surface of metals. This study also deal with how to enhance the wear resistance, corrosion resistance, hot gaseous corrosion resistance. Furthermore, literary text about the hardness improvement by upgrade the service life component. It gives Information about which type of welding process is prominent or optimal for hard-facing.

M.F Buchely *et al.*[1] An investigation was made to think about the microstructure and scraped area opposition of hard-facing compounds fortified with essential chromium carbides, complex carbides or tungsten carbides. Base metal was ASTM A36 Carbon steel plates. Shielded metal arc welding was used. Three different electrodes were used. Abrasion test was conducted by rubber wheel using dry sand abrasion machine. Microstructure was studied by SEM and optical microscope. Two layers of hard-facing with chromium rich electrode, Single layer of weld with W-rich electrode and three layers of hard-facing with complex carbides electrode were deposited.

Table 2.1 Process parameters for SMAW

Electrode	Velocity (mm/min)	Current (A)	Voltage
Chromium Rich	190-200	130	20-23
Complex carbides	180-200	200	25-30
W-Rich	180-200	175	20-23

\W-rich layer of hard-facing was showed good behavior of wear resistance with single weld layer due to the formation of eutectic matrix combine with carbides (M_7C_3 and MC). M_7C_3 carbide prevented from cutting and cultivate by abrasive particle. Complex carbides of three layers presented a very elegant abrasive wear

resistant and single layer diminished the wear resistant because deposited alloy highly diluted in base metal and change the size of microstructure.

V.E. Buchanan *et al.* [2] used grey cast iron as base material. SEM operation and optical technique used to study the grains structure. Wear test operated by block on ring technique. Two types of electrodes were used which are coated with hypereutectic and hypoeutectic materials. Diameter of electrodes were 3.2mm and 4 mm respectively. Welding technique was submerged arc welding (SMAW). No preheating technique used before welding. Substrate kept at ambient temperature After the welding operation. Current parameter for both type electrodes were 125A and 145A respectively. There was distinction in the hardness of both materials but no clue about wear resistance which was superior. Mass loss is directly proportional to sliding distance but not with load. Due to the formation of M_7C_3 carbides in hypereutectic gave a powerful hindrance to furrowing and cutting of rough abrasive particle yet under pressure the carbides were broadly cracked.

Jibo Wang *et al.*[3] this study show that impact of nitrogen added substance on the microstructure and rough effect wear opposition of hard-facing amalgam with high chromium. Hardness estimated by nano-indentation test of carbides. Open arc welding technique was used. It take three types of alloys one with no addition of nitrogen and others two have the values of nitrogen addition were 0, 0.09wt% and 0.19wt%.The hardness is expanded somewhat from 18.7 GPa to 21.3 GPa, with addition of nitrogen. Wear Test performed also in which volume loss diminish from 72 mm³ to 39 mm³. Carbides were fractured without nitrogen addition. Grain size was refined due to addition of nitrogen. Amid the effect rough wear test process, the volume loss of 0.19wt% nitrogen addition alloy is expanded with the expansion of hardness, estimate, speed what's more, affected point of the grating particles. Due to large size grain size of hard-facing alloys in which no addition of nitrogen content got easily cracked and no gain of impact energy during wear test but 0.19wt% show great wear resistance due to small size of grain size ,no cracks occurred and absorb the impact energy due to bending of carbides.

Junfeng Gou. *et al.* [4] in this study nano particles of rare earth oxide added in hard-facing alloys. Different content of REO added in flux cored wire. Three wires were prepared with different composition of REO. Weight fraction of REO were 0 wt% , .288 wt%, 0.576 wt%. Different technology used to study about behavior of

the REO. Optical microscope and SEM were utilized to watch the microstructure of the Fe-based hard-facing combinations. XRD was utilized to contemplate the phases of the hard-facing composites. Spectroscopy used to study the hard-facing alloys and Pin-On-Disc test performed also. Rare earth oxide (REO) nanoparticles was refined the essential carbide. The territory of essential carbide in the hardfacing compound without REO nanoparticles was $828.75 \mu\text{m}^2$. The territory of essential carbide in the hardfacing composite with 0.288 wt% REO nanoparticles was $406.25 \mu\text{m}^2$. Bending strength improved by 46.4% than hard-facing alloys with no addition of REO. Wear resistance increased with the addition of REO. 0.288wt% REO has greater wear resistance than other two hard-facing alloys. Mechanisms of wear were abrasion and mild oxidation wear when load was 5N and when load was 30 N then mechanism were severe oxidation and abrasion wear.

Hao Wang *et al.*[5] studied that cast iron with high chromium content deposited on low carbon steel with the help of electro slag welding. Mixture was heated at different temperature. After the heat treatment microstructure was studied in favor of hardness and wear resistance. Cast iron with high chromium layer deposited on low alloys steel and after welding specimen heated at 520°C is known as post weld heat treatment (PWHT). If PWHT at 520°C compare with the welding sample, Hardness and wear resistance expanded by 11.88% and 25% due to formation of Primary carbides (M_{23}C_6) and Martensite. Wear obstruction and hardness decreases due to pearlite. Wear performance was high of PWHT at 520°C after welding of HCCI on low alloys steel, cracks occurred upto $2 \mu\text{m}$ in depth.

Farzad Sadeghi *et al.*[6] studied that effect of tantalum on microstructure and wear resistance. Tantalum replace with niobium to refine grain structure. Welding technique was gas tungsten arc welding. Addition of niobium had no effect on microstructure of base metal and eutectic content and dendrites of austenite shown with addition of niobium. Base metal selected as low carbon steel. There were three phase zone observed by optical microscope. Zone I was of base metal. It contained mixture of austenite and martensite. Zone II The second zone showed a hypoeutectic microstructure containing essential austenite dendrites and eutectic constituents. Wear resistance provide by Zone III. Addition of Niobium made no change in microstructure. It was same as base metal. Due to addition of Tantalum microstructure has changed. M_7C_3 Carbide present in matrix of eutectic. Hardness Value expanded

from 46 HRC to 55 HRC. Niobium with vanadium increased hardness due to formation of eutectic content and maximum value of hardness 64 HRC with tantalum addition due to formation of M_7C_3 Carbide. Reciprocating wear resistance enhanced by Tantalum.

Yinping Ding *et al.*[7] used hard-facing of stellite alloys composition to improve the hardness and wear performance of control valve seat. Laser cladding technology was used for hard-facing. Base metal stainless steel was used. Stellite 3 was 70% and satellite 21 was 30%. Microstructure studied via SEM, XRD and EDS. Liquid penetrating test was used to check cracking. stainless steel did not show any cracks. Corrosion test performed in morpholine solution which had 9.5 ph value. Cavitation erosion occurred in NAOH solution. Stellite 3 and satellite 21 alloys mixture had large volume fraction of carbides that's why it provided high hardness and better wear resistance. Stellite 6 performed better pitting corrosion resistance with less volume of carbides presented. Carbides react more electrochemical reactions. Both satellite 6 and satellite alloy mixture produce Cr_2O_3 layer. It prevent the base metal from corrosion and cavitation.

Manel Rodríguez Ripoll *et al.*[8] used high power direct diode laser for hard-facing of high speed steel as base metal. Niobium used in powder form. Quantity of Nb varied from 0.1% wt, 1% wt and 3% wt. Niobium has great effect on grain structure and its mechanical structure. Particle size of niobium was 74 μm . Polyethylene glycol dodecyl ether was used as a binder to mix the powder. HSS plates had own hardness of 150 HV30. Energy of laser was 4.5 Kw. There was change in microstructure with addition of different contents of niobium. Amount of carbides reduced as increase the amount of niobium content. The chances of failure reduced due to increase of elastic strain. It enhanced the toughness and corrosion resistance also. Erosion resistance had not improved by niobium content.

F. Molleda *et al.*[9] used soft carbon steel as a base metal. Manganese with high content deposited on this base metal with the help of electrode. Many problems were occurring in homogeneous joint like corrosion and interface wear. In heterogeneous materials were diffused in liquid filler metal during deposition with electrode. Corrosion resistance arise as chemical composition vary. Electrode contained large carbon content and it affect the interface zone. Martensite band were seen near the

interface zone. It arise the brittle nature and failure to tolerate dynamic loading. Carbon content diffused from filler material to base metal.

J.B. Wang *et al.*[10] studied the impact of nitrogen added substance on the microstructure and mechanical properties of martensitic treated steel hard-facing was examined in this work. Phase Examined by XRD. Microstructure studied by FESEM (field emission scanning electron microscope) and TEM (transmission electron microscope) for both hard-facing nitrogen additive and without nitrogen addition. Flux cored wire fabricated with rolling process. External shell of flux cored wire was the low carbon steel strip of H08A. Base metal was Q235 steel. Submerged arc welding technique was used. Five layers were deposited on steel substrate with welding technique. In hardfacing by substitute the nitrogen instead of carbon refined the grain austenite size. It improve the ductility and change the brittle nature of hard-facing to ductile transgranule. Yield strength expanded from 884 MPa to 996 MPa. Rigidity expanded from 1078 MPa to 1554 MPa.

Tadeusz Hejwowski *et al.*[11] In the present paper, the capability of surface coatings to build erosion of IC engine valves is examined. The corrosion tests were completed to contemplate in reproduced engine chamber condition the execution of Ni-, Co-and Fe-based materials utilized for plasma deposition. Hot corrosion tests were performed in air, sulfur dioxide containing environment and in liquid manufactured synthetic. The crucible arranging test was utilized to reproduce stores on valve seats from residual fuel burning which are in charge of quick consumption because of the nearness of liquid stage. The new combinations containing Ni and Co can be conceivably connected as valve hard-facings. It was found in the tests completed in air, sulfur dioxide and in synthetic debris that experimental alloys, in which Co was mostly supplanted by Ni, seemed to have potential as valve hard-facings. They beat grade 6 stellite regularly connected to valve seats. The connected new alloys ought to contain direct substance of Co i.e. about 30 wt%. Results additionally vouch for advantage of wide utilization of hard-facings to ensure valve steel against corrosion assault of species contained in ignition gases.

Yogesh Kumar Singla *et al.*[12] This study revealed that built a hard-facing layer via pre placement technique. Pre placement technique defined as place the powder on substrate before welding. Shielded metal arc welding was used. In this investigation, compare the mechanical and tribological properties between niobium additive hard-

facing alloys and without addition of niobium in hard-facing alloys. Optical microscope used to study the microstructure. Xrd was shown that which type of carbide was formed. Wear test was performed by pin-on-disc instrument. Weight loss occurred in niobium additive was 0.0024 g and weight loss in niobium free hard-facing alloys was 0.0064 g. Niobium addition with 0.4 wt% show good wear resistance. Wear resistance was expanded by 2.64%. Niobium addition was increased the hardness value of hard-facing alloys. It was reached to peak value of 751.66 VHN.

Yogesh Kumar Singla *et al.*[13] In this paper single investigated the effect of content of rare earth oxide on microstructure , mechanical and tribological properties. Four hard-facing layer was deposited with different wt% of cerium oxide that was 0 wt % , 2 wt% , 4 wt% and 6 wt%. This study revealed that mechanical properties and microstructure was not improved with raise the wt% of rare earth oxide. Grain size was decreased with addition of 2 wt% and 4 wt% but it was reduced at 6 wt% content of ceO_2 . Grains were smaller in size then more was the hardness. Highest peak of hardness 699.52 VHN was shown in 4 wt% ceO_2 . Phase transformation was not occurred. Weight percentage was shown no effects on carbides. Wear resistance of 6 wt% content was poor. Wear resistant of 4 wt % content of reo was best. This study was shown that with increase in the content of wt% of reo, Hardness was reduced and grain size was became large. Wear resistance was got diminished.

YANG Dong *et al.*[14] Impacts of La expansion on corrosion resistance of hot-dipped galvalume covering steel wire were researched. The consumption opposition of Zn-Al-Si-La alloys coatings containing 0, 0.02 wt.%, 0.05 wt.%, 0.1wt.% and 0.2wt.% La were assessed by different tests, for example, copper-quickened acidic corrosive salt splash testing (CASS), drenching test in 3.5% NaCl solution, electrochemical tests including weak polarization bends and electrochemical impedance spectroscopy (EIS) tests, Scanning electron microscopic (SEM) test and X-ray diffraction (XRD) test. It was discovered that the erosion opposition of galvalume covering could be enhanced by including accurate measures of La. Then, the mechanism of the change of erosion obstruction by La expansion was talked about. La with 0.05wt% was shown best corrosion resistance. With addition Lanthanum, number of oxygen present in the alloys was reduced.

2.15 F. Cajner *et al.* [15] Nitriding builds surface hardness and enhances wear resistance of stainless steels. Many times, nitriding can diminish the corrosion

resistance. In this paper, the impact of nitriding on the corrosion resistance of martensitic pure steel was examined. Plasma nitriding at 440 °C and 525 °C and salt spray nitrocarburizing were completed on X17CrNi16-2 stainless steel. Microhardness profiles of the nitrided layers were analyzed. Phase organization examination and quantitative depth profile examination of the nitrided layers were performed by X-ray diffraction (XRD) and glow discharge optical emission spectrometry (GD-OES), separately. Corrosion behaviour was observed by immersion test in 1% HCl, salt splash test in 5% NaCl and electrochemical corrosion tests in 3.5% NaCl salt solution. Results demonstrate that salt shower nitro carburizing and plasma nitriding at low temperature, expanded microhardness without descending the corrosion resistance. Plasma nitriding at a higher temperature expanded the corrosion tendency of the X17CrNi16-2 steel.

CHEN Yan *et al.* [16] As-cast Cu-La alloys with La substance in the scope of 0–0.32 wt.% were created by vacuum melting technique. The impacts of La on microstructure and mechanical properties of pure copper were examined utilizing optical microscopy (OM), scanning electronic microscopy (SEM), transmission electron microscopy (TEM), X-Ray diffraction (XRD) and tensile test. The outcomes appeared that La affected the hardening microstructure and the grain refinement of as-cast pure copper. With the expansion of La content, rigidity, the yield strength and the micro-hardness expanded, however the lengthening expanded in the first place and afterward diminished when La content above 0.089 wt.%. The change of mechanical properties was ascribed to the impact of grain refinement and purifying. However, extreme including La would fall apart the elongation owing to the Cu₆La stages.

Yogesh Kumar Singla *et al.* [17] In this study it was investigated that the effect of addition of three different contents of vanadium in hard-facing alloys on microstructure, wear resistance and macro-hardness of weld bead. Mild steel was selected as base metal. Shielded metal arc welding was used. Alloys were added in weld deposition through pre placement method. This study was revealed that with increased the content of vanadium improve the hardness and reduce the weight loss during wear. Wear test performed by pin on plate instrument. Vanadium with 1.5 wt% content had V₈C₇ and VC particles which were very hard. Alloys with 0 wt% and 0.6 wt% content of vanadium have not any hard particles. Vanadium content of 1.5 wt%

improved the mechanical properties and wear resistance. Grains structure of weld bead also refined due to presence of hard particles.

Yogesh Kumar Singla *et al.*[18] This research was revealed that addition of chromium to the hard-facing alloys, improved the grains structure and wear resistance. Low carbon mild steel was selected as base material. Shielded metal arc welding was used for deposition of hard-facing alloys. Microstructure was studied by optical microscope and scanning electron microscope. Pin on disc machine was used to study the wear resistance. Six different hard-facing with different chromium content was prepared. Hard-facing with high chromium content was shown good wear resistance. Number carbides were detected by optical microscope. With increase in chromium content, numbers of carbide were also increased. These carbides were looked like long spine like blade. These carbides were M_7C_3 .

CHAPTER3

PROBLEM FORMULATION

Hard-facing is advance technique for development of surface of material to enhance its properties like hardness and wear. This technique is done by welding or thermal spray etc. It improves the dimension of worn part of machine. Mainly hard-facing is very cheap and low cost method to improves or repair the wear part of machine. With the help of welding, hard-facing is done. It has many applications in industries like sugarcane roller, rock crusher, Crane jaws, turbine blades etc.

Problem associated is to investigate the wear and corrosion behavior of hard-facing elements formed by addition of lanthanum oxide and hexa boron nitride by manual arc welding

Objective

To enhance the above mentioned properties, an experiment was used to deposit layer of hard-facing on the substrate by manual arc welding. The aim of experiment was to improve the microstructure, hardness, wear resistance and corrosion resistance. For this purpose, hard-facing layer was deposited by addition of HBN and La_2O_3 on substrate with manual arc welding process. Experiment was performed on wear test, micro-hardness, corrosion test and EBSD to study the microstructure.

1. To study the effect of Lanthanum oxide on wear resistance and microstructure of weld bead.
2. To study the effect of HBN on wear resistance and microstructure of weld bead
3. To study the effect of combination of HBN and lanthanum oxide on wear resistance and microstructure of weld bead
4. Above three Sample also used to study the corrosion resistance

CHAPTER4

METHODOLOGY

4.1 INTRODUCTION

During this experimentation, different powder form of alloys was used during hard-facing with manual arc welding process. Parameters of welding process remain constant during hard-facing of all samples. Following steps performed during experimentation :

- (a) The First step was preparing of alloys combinations which are used to diffuse in base metal viz. hexa boron nitride, Lanthanum, Lanthanum and hexa boron nitride.
- (b) The Second step was machining of low carbon steel plate (mild steel) having dimension $125 \times 25 \times 10$ mm³. Groove was machined to carry the powder form of alloys otherwise powder was flown out during welding.
- (c) The Third step set up the welding set for fabricating the hard-facing layer on steel plates by use of different alloys
- (d) The fourth step was prepared the samples for different experiments. Manufacture the size of specimen according to the requirement of machine.

4.2 Types of test performed are given as follow:

- ❖ Micro-hardness
- ❖ EBSD 3d
- ❖ Corrosion test
- ❖ SEM
- ❖ Wear test
- ❖ Spectroscopy

4.3 Material used as base metal

Mild steel of grade E-250 of $125 \times 25 \times 10$ mm³ dimensions were prepared for welding. This metal was chosen because it has wide applications in industries like steel frame building, machinery parts and pipelines. It is cheaper than other steels. Mild steel has combination of iron and carbon but content of iron is more than carbon. Steels which contain high content of carbon get easily crack and break under suddenly applied load but mild steel has high deformation and bending strength.

Table 4.1 Material composition of mild steel of grade E-250

Alloys	Iron (Fe)	Manganese (Mn)	Silicon (Si)	Carbon (C)	Phosphorus (P)	Sulphur (S)
Wt %	99.248	0.281	0.225	0.201	0.018	0.027

4.4 Prepared the specimen for welding

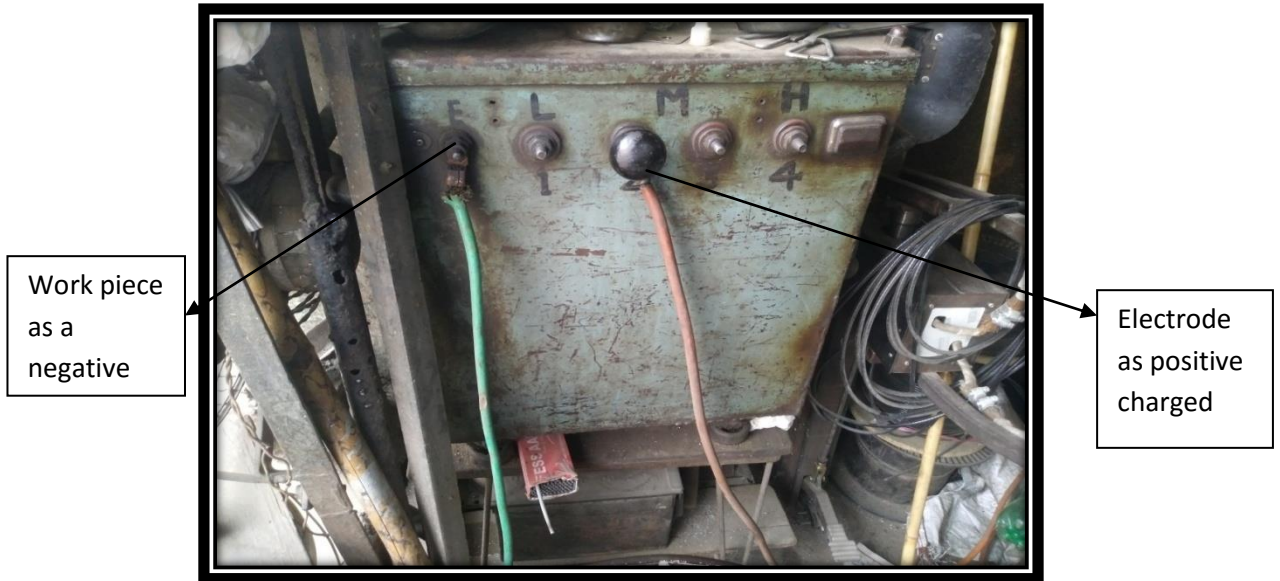
Manufacturing of steel plate whose dimensions are 125×25×10 mm³. A groove was manufactured with the help of lath machine. This groove was placed at centre of plate in longitudinal direction. It helps to hold the powder during welding because powder was blown out with gaseous of welding electrode. Depth of groove was 3 mm and width was 6 mm. With this groove very small content of powder was volatile with flue gaseous.



Figure 4.1 Steel Plates with groove (Courtesy: Behra road Patiala)

4.5 Manual arc welding set

Manual arc welding set was used for deposition of hard-facing layer. Step down transformer was used to convert the alternate current into direct current. Reverse polarity was used as principle. It means electrode act as positive and work piece act as negative. DC is used to produce an electric arc between workpiece and electrode. A pool of molten metal was formed to join two surface of metal. Electric arc is produced by little bit touch of electrode with workpiece. Arc initiated after small touch, then flux of the electrode passed to molten metal. Slag was formed on the surface of weld bead protect it from oxygen and surrounding gases.



Work piece
as a
negative

Electrode
as positive
charged

Figure 4.2 Manual arc Welding Setup (Courtesy: Harmindra workshop patiala)

4.6 Welding parameter

Welding parameters were remained constant for each hard-facing layer. DC voltage was applied. Velocity of weld deposition was measured by counting the time with stop watch. It was 28 second for every weld bead. Length of steel plate was 125 mm. Velocity was calculated by distance/time.

Table 4.2 Welding Parameters

Voltage (V)	Current (A)	Weld travel velocity (mm/sec)
43	150	4.64

4.7 Welding Electrode

A medium heavy coated rutile type electrode used for hard-facing application on mild steel, carbon steels and low alloy steels. It has its own hardness of 250 BHN (approx) after deposition of two hard-facing layers. Size of electrode was 3.15 mm in diameter. These electrodes are use in wide application like gears, shafts, coupling, sugarcane, crushers, axle hammers etc. Length of electrode was 450 mm.



Figure 4.3 Electrodes used for hard-facing

Table 4.3 Electrode Composition of alloys

Alloys	Carbon (C)	Manganese (Mn)	Silicon (Si)	Chromium (Cr)	Molybdenum (Mo)
Composition in wt%	0.15	0.40	0.25	0.70	1.00

4.8 Preparation of manual arc welding process

The material was distributed in groove of base metal. Total volume of groove completely filled with powder and compressed the powder with scale to make uniform thickness. Clamp the specimen in tool holder in order to produce uniform layer of weld bead.



Figure 4.4 groove filled with powder (Courtesy: Harmindra workshop patiala)

Weld bead of thickness 5 to 6 mm were deposited with help of rutile type electrode. Powder was completely diffused in the steel plate. Moisture content of powder was volatile with high temperature of electrode.



Figure 4.5 Weld bead (Courtesy: Harmindra workshop patiala)

4.9 Powder used as ingredients

- **Hexa boron nitride** of grade HCV and white in color. Its crystal was turbostratic. Crystal size vary from 0.1-0.2 μm . Mean particle size for the fine powder was 7-11 μm . It contains 0.05% of carbon.
- **Lanthanum oxide** (Rare earth oxide) used in powder form .Properties and results of this samples was compared with hexa boron nitride.
- Third specimen was prepared with combination of both the powders lanthanum oxide and hexa boron nitride.
- Fourth specimen was prepared with no alloys addition. It was just welded with rutile type electrode without addition of any alloys.

Table 4.4 Samples Weight percentage

Sample	Wt%
Sample A	No alloy was added. Deposition of weld bead with only rutile electrode
Sample N	0.68 wt % of HBN + rutile type electrode
Sample LN	0.21wt% of La_2O_3 + 0.21wt% HBN + rutile type electrode
Sample L	1.1 wt% of La_2O_3 + rutile type electrode

4.10 Following experiments were performed on specimen to achieve the results

4.10.1 Micro hardness Test

Micro-hardness testing was done on weld bead of samples. Load kept constant for all four samples. Load taken was 500 gram. Dwell time was 20 seconds for all samples. It was taken 20 seconds for indentation.

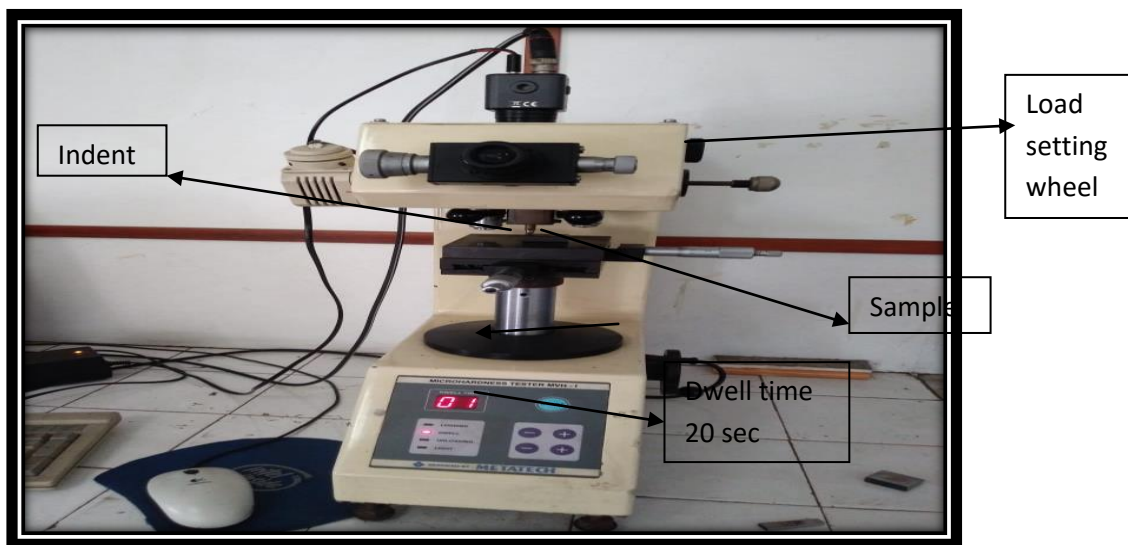


Figure 4.6 Micro hardness testing machine (Courtesy: Advance metallurgical lab tict Patiala)

Surface of the samples for hardness testing became flat with surface grinder. After grinding, samples were polished with abrasive paper of 100, 200, 300, 600, 800, 1000, 2000 and 3000 grit size with the help of polished machine. After polished, weld bead of samples were observed clear. Indenter was taken 20 seconds for loading and 20 seconds for unloading.

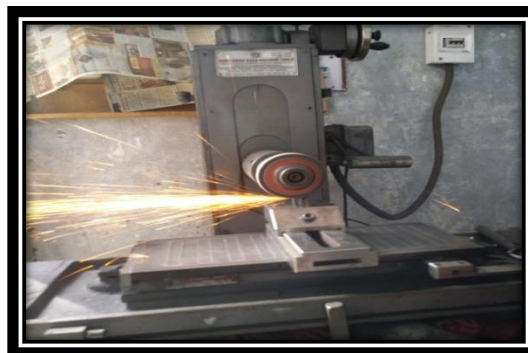


Figure 4.7 Surface grinder (Courtesy: Harmindra workshop patiala)

4.11 Disk Polisher Machine

Disk polisher machine has two types of wheel one is used to install grit paper and other is used for velvet cloth. Abrasive paper was rotated on wheel of disk polisher with help of motor. Velvet cloth was removed the dust and debris from sample. It was provided mirror like finish on surface of metal which was rubbed on abrasive paper.



Figure 4.9 Disk polisher (Courtesy: Machine tool lab tiet patiala)



Figure 4.10 Sample after polishing (Courtesy: Harmindra workshop Patiala)

4.12 EBSD (Electron Back Scattered Diffraction)

Ebsd test was used to study the crystallographic orientation. It provides information about phase formation and orientation of crystallographic crystal. Sample was

prepared for ebsd 3d testing was $10 \times 10 \times 10 \text{ mm}^3$ in size. Before the test was performed, sample should be polished. So, sample was polished by electropolishing machine. Electropolish was done by passing the current of 4.5A at 27 V for 10 seconds. Electrolyte was used for electropolishing was 80 percent methanol and 20 percent perchloric acid. It remove layer of material and enhance the mirror like finish.



Figure 4.10 Electropolishing machine (courtesy iit bombay)



Figure 4.11 Samples after electropolishing (Courtesy: iit bombay)

4.13 Salt spray chamber for corrosion test

Salt spray chamber was used to perform corrosion test. It corrode the metal at very rapid rate. ASTM-B-117 method was used to study the corrosive nature of weld bead. Nacl salt solution passed through samples by using pressurized air. Concentration of Nacl salt solution was 5%.

Table 4.4 Parameters during corrosion test

Ambient Temperature	29±2 °C
Relative Humidity	95±2%
Conc. Of Nacl solution	5%
Time	0-120 hours



Figure 4.12 Salt Spray Chamber (Courtesy alpha test house mohali)

4.14 SEM (Scanning Electron Microscope)

A Scanning Electron microscope (SEM) is a kind of electron magnifying lens that produces pictures of an sample by examining the surface with an engaged light emission. The electrons associate with atoms in the sample, creating different signs that contain data about the sample's surface structure. SEM used to study about the microstructure of material. Grain orientation information and grain boundaries described by SEM machine.



Figure 4.13 SEM machine (Courtesy: SAI lab tiet patiala)

4.15 Wear test performed on pin-on-disc machine

Wear test was performed by pin on disc machine. Sample size of $10 \times 10 \times 10 \text{ mm}^3$ was used. Weld bead of samples has relative motion with disc to study the wear nature. Each weld bead has constant cross section area to obtain uniform wear. Here Sample was used as pin are following:



Figure 4.14 Samples for wear

4.15.1 Material used for disc

EN31 grade of steel was used to manufacture disc. Hardness of disc was 58-62 HRC after tempered. Disc was polished by surface grinder. diameter of disc was 100 mm and thickness was 8 mm.



Figure 4.15 Disk of EN 31 steel grade

4.15.2 Weigh Machine

Prescribed weighing machine was used to measure weight loss of wear sample after run on machine. Least count error was 0.001.



Figure 4.16 Weigh machine

4.15.3 Pin-on-Disc Experiment

A tribometer is an instrument that measures tribological amounts, for example, coefficient of rubbing, grinding power, and wear volume, between two surfaces, which were in contact. Two types of loads was used 5kg (49.05 N) and 7.5kg (73.575 N). Single speed of 2 m/s was set. It was ran on different sliding distance of 600 m, 1200 m ,1800 m, 2400 m, 3000 m, 3600 m , 5400m and 6000 m.



Figure 4.17 Pin on disc machine (Courtesy: Machine tool lab tiet Patiala)

CHAPTER 5

RESULTS AND DISCUSSION

5.1 Electron backscatter diffraction

EBSD recognizes the types of phases in the material. Grain size has great significance on mechanical properties of material. EBSD is technique to predict the grain size, grain boundaries and Orientation of crystallographic structure. It provides the advance information of grain size and types of boundaries. In this Analysis different color shows the different orientation. One color is considers as one grain.

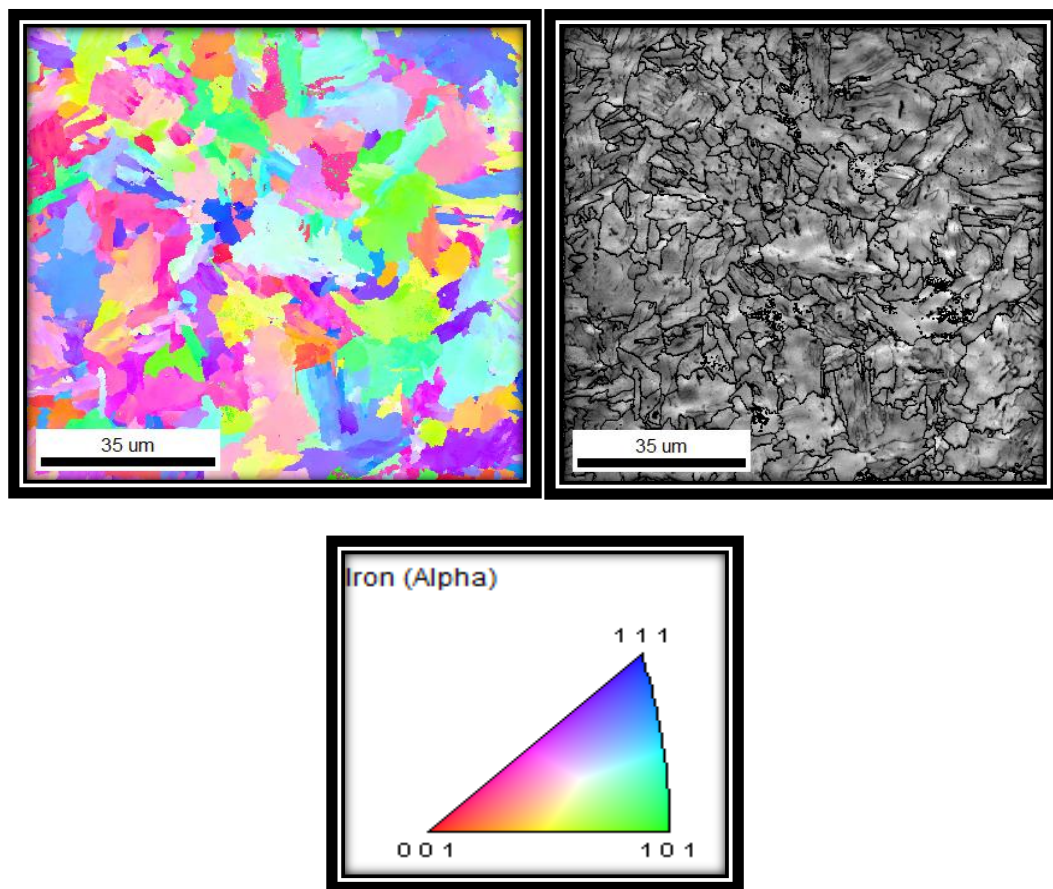


Figure 5.1 EBSD map and inverse pole figure of sample A (Reference)

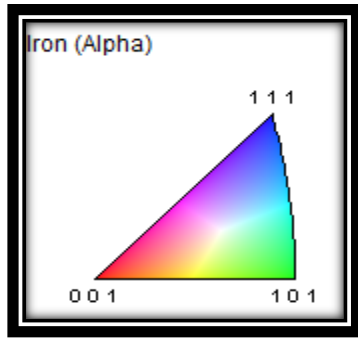
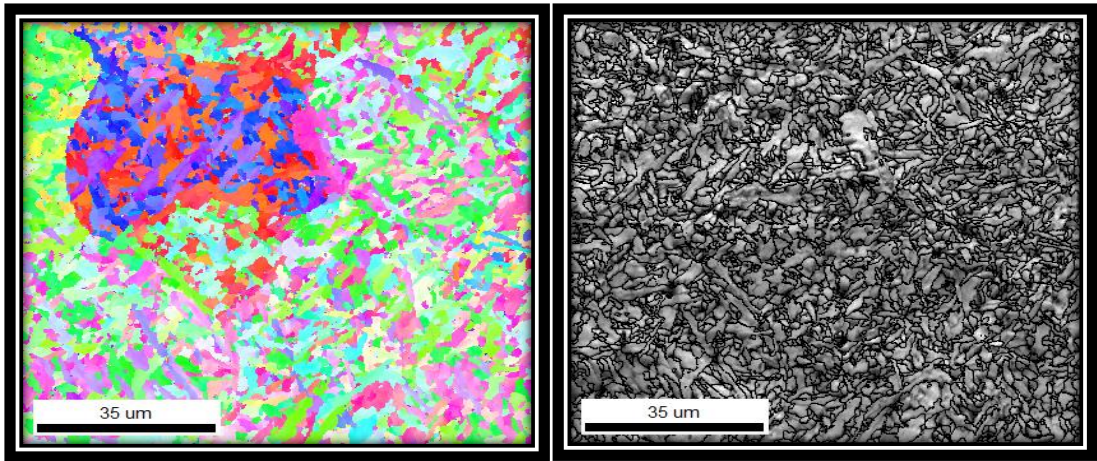


Figure 5.2 EBSD map and inverse pole figure of sample N

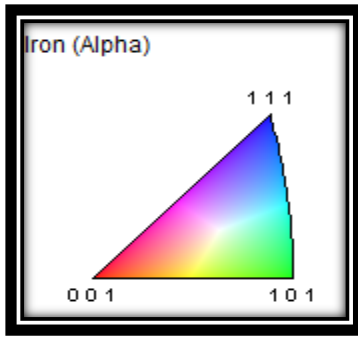
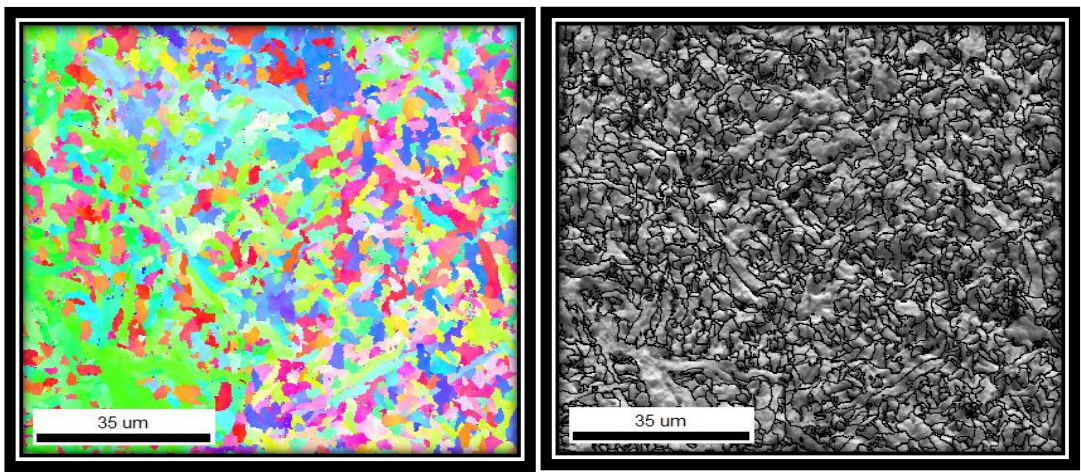


Figure 5.3 EBSD map and inverse pole figure of sample LN

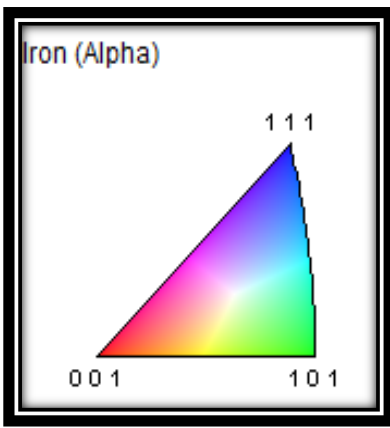
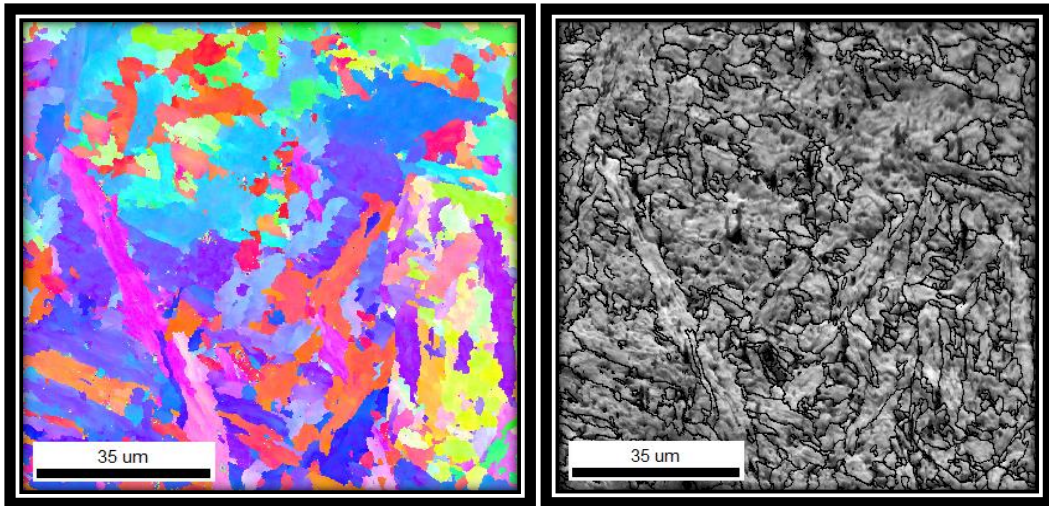
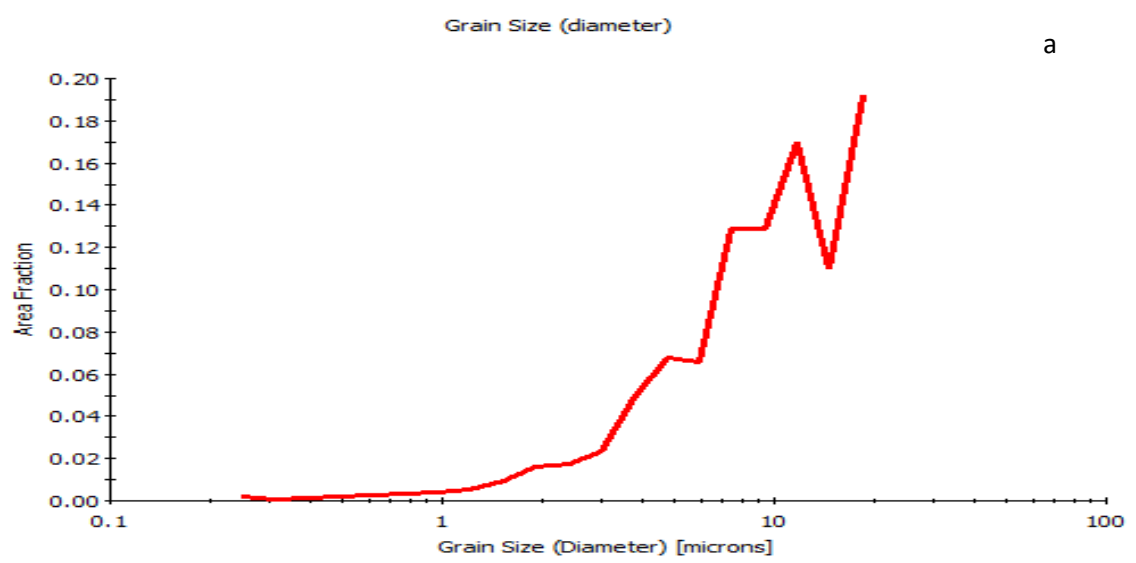


Figure 5.4 EBSD map and inverse pole figure of sample L



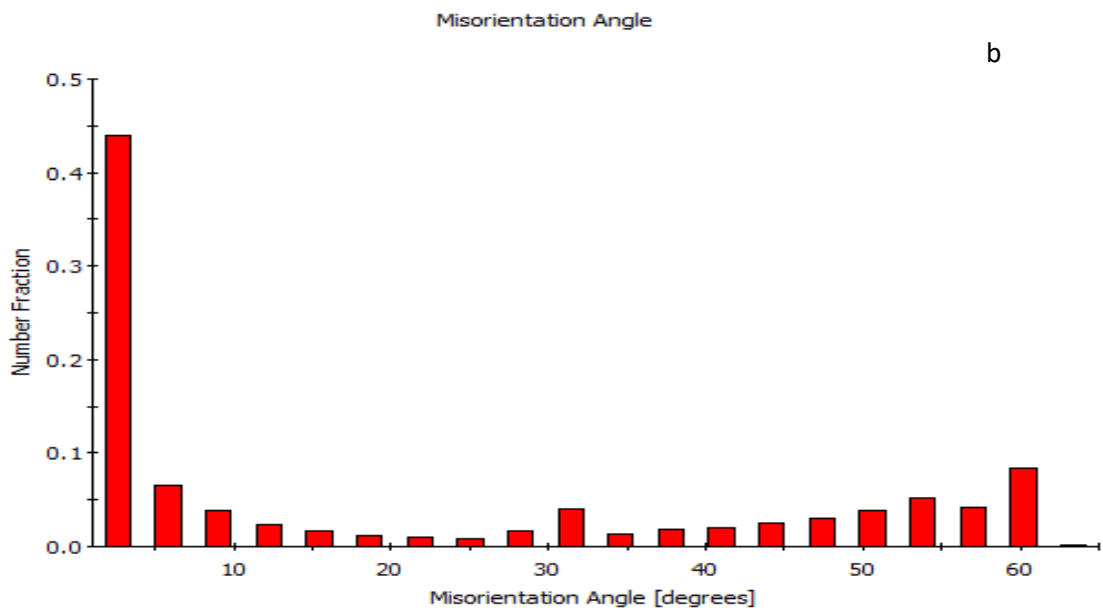
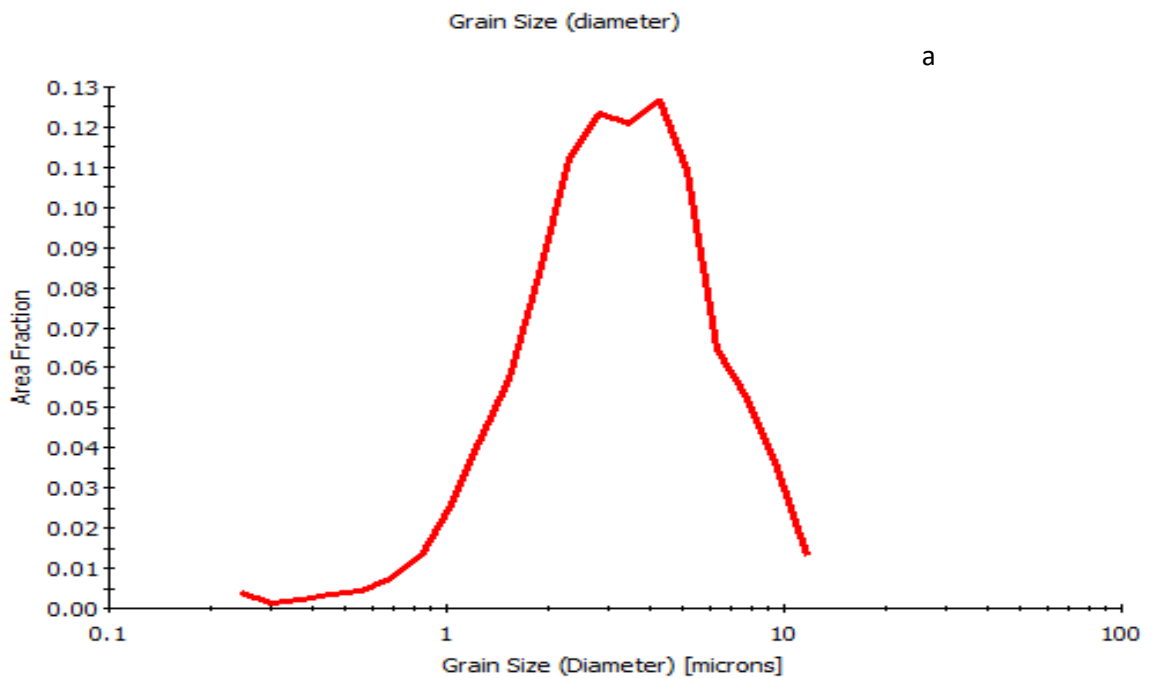


Figure 5.5 (a) EBSD map of grain size distribution with area fraction (b) Grain misorientation distribution on the top surface of weld bead of sample A



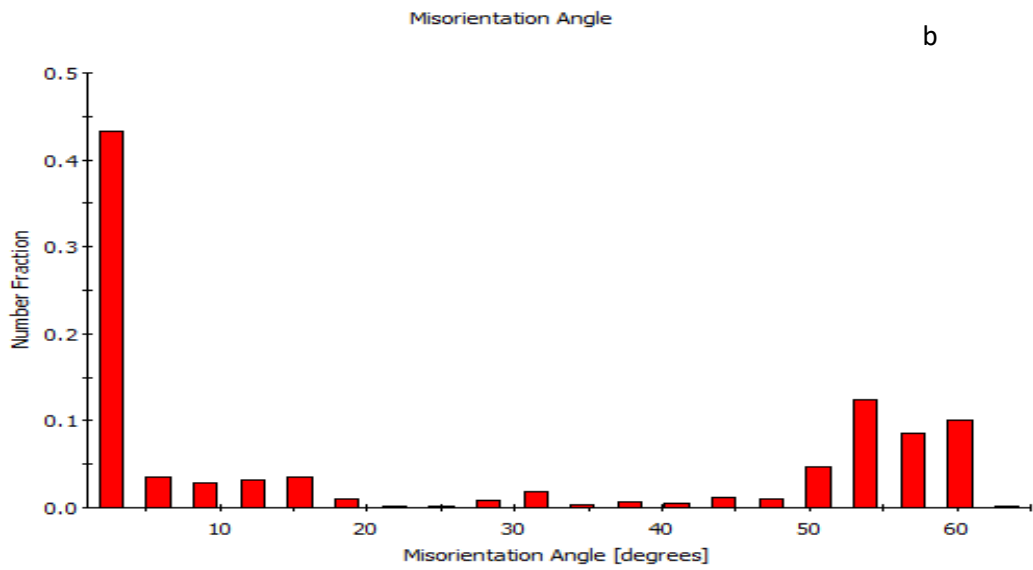
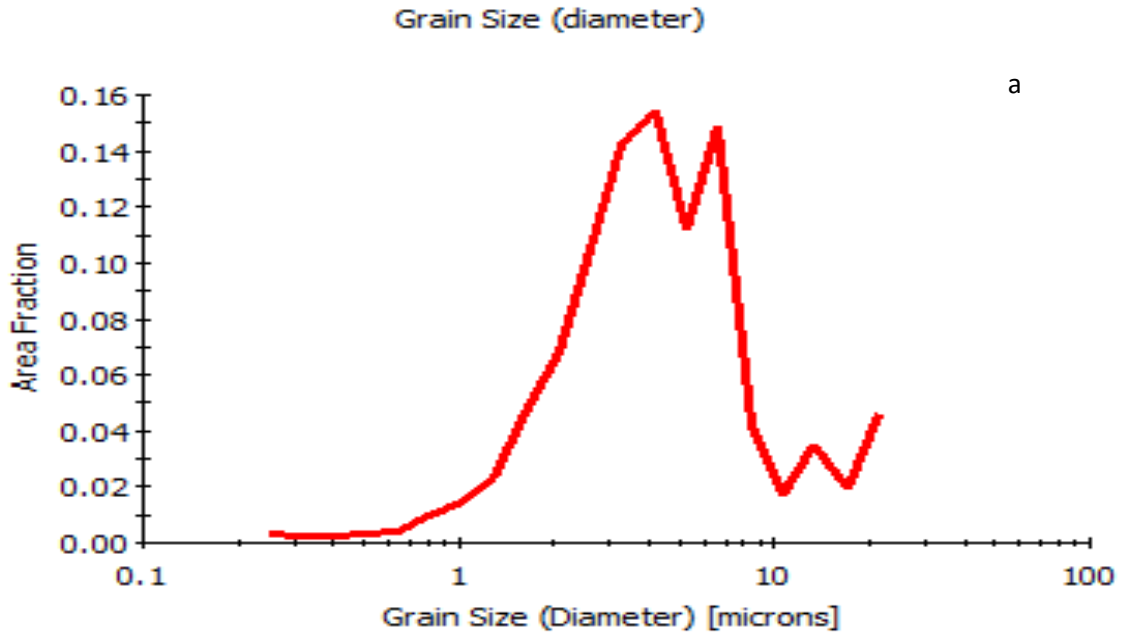


Figure 5.6 (a) EBSD map of grain size distribution with area fraction (b) Grain misorientation distribution on the top surface of weld bead of sample N



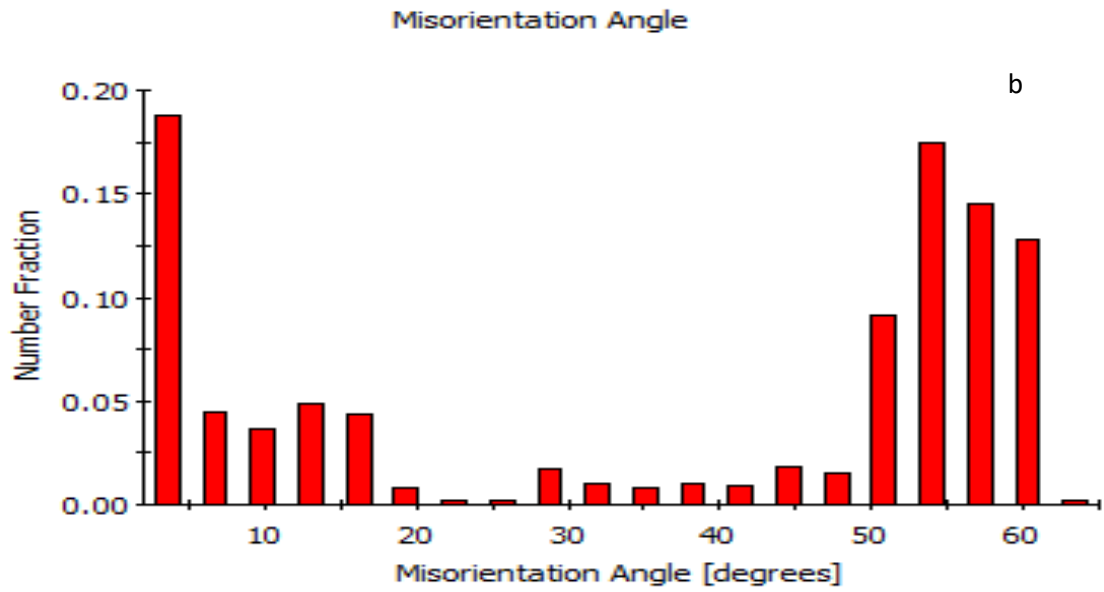
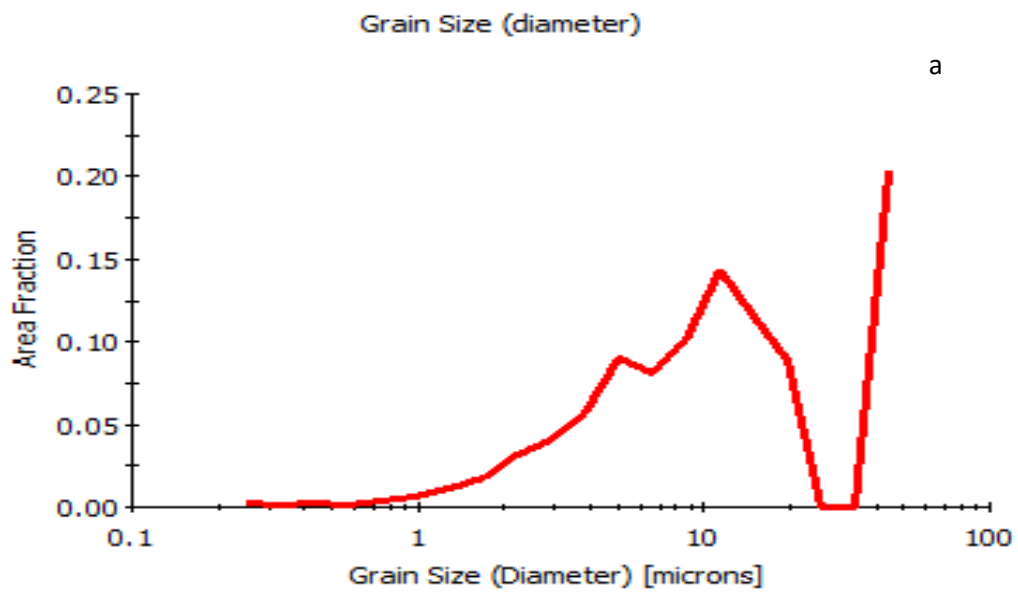
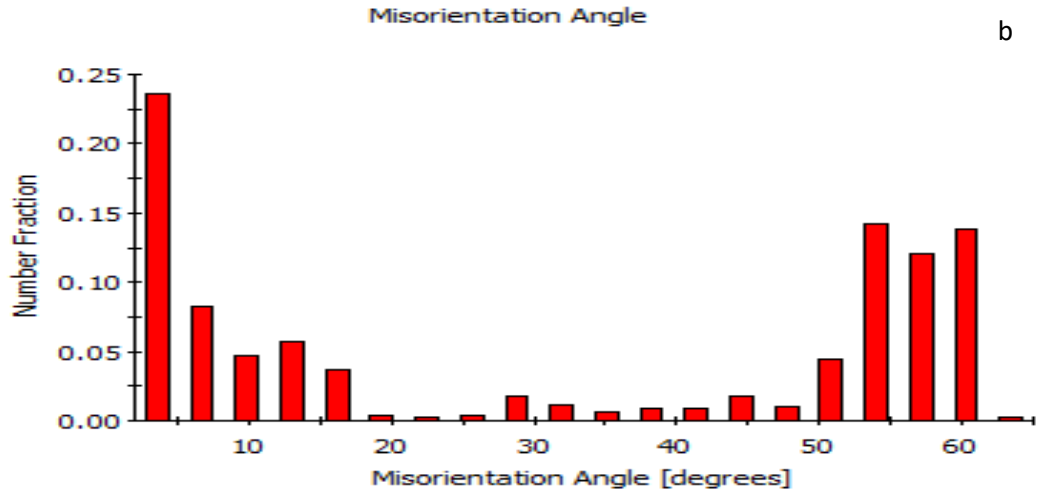


Figure 5.7 (a) EBSD map of grain size distribution with area fraction (b) Grain misorientation distribution on the top surface of weld bead of sample LN





5.8 (a) EBSD map of grain size distribution with area fraction (b) Grain misorientation distribution on top surface of weld bead of sample L

Discussion of EBSD maps

(a) Sample A

It was formed BCC structure and Iron (alpha) phase was formed. Homogeneous structure was observed because each grain had same orientation. Average Grain size was 10.5847 μm . More twin boundaries were formed due to recrystallization at low boundary angle 5° and at 60°. Twin boundaries are those which have sharp edges. Inverse pole figure helps in visualize the texture. It was easy to observed that which crystal lies parallel to the surface of sample. (100) denote the face of the crystal parallel to surface, (110) denote that edge of the crystal parallel to the surface and (111) denote the corner of crystal parallel to the surface. From figure 5.5 (a) was revealed that grains with diameter 0.249459 micron was covered less fraction of area that was .00213397. With increase in the size of grains, area fraction was increased. Largest size of grains was 18.4321 micron, which were covered the most fraction of area. Trend was changed at grain size of 14.597 micron, which was covered 0.109518 area fraction. From figure 5.5 (b) observed that 0.440315 grains were misoriented at 2.6° angle. Misorientation angle means that two grain boundaries were inclined at some angle. 0.00908281 numbers fraction of grains have 25° misorientation angle. It was shown clear from Figure 5.5 (b) that large numbers fraction of grains were misoriented at smaller angle and few grains were misoriented at higher angles 25° and 63.4° angles.

(b) Sample N

There was no precipitate of hexa boron nitride was formed. Homogeneous solution is formed. Uniform grain size is observed. Average grain size was $3.78214 \pm 2.3514 \mu\text{m}$. It was shown more twin boundaries in microstructure at low boundary angle less than 5° and high boundary angle 60° . Grain size with smaller size was oriented in same direction and grain with larger in size was oriented in other direction but in same pattern. Small size grains were large in numbers. It was form Iron (alpha) phase and BCC structure. From figure 5.6 (a) observed that with increase in the size of grains in diameter (microns) fraction of area was increased. Small grains with diameter 0.246559 microns has covered less area fraction 0.00402211. Area fraction increased with grain size upto 4.23723 micron diameter and area fraction was 0.126981. It was the highest fraction of area covered by this size of grains. After that trend was changed now Area fraction was start to decreased with increase in size of grain diameter. Larger grains size 11.7005 microns covered 0.0132781 area fraction

(c) Sample LN

Grains structure uniformly oriented. It had Large number of twin boundaries. These boundaries form during the phase transformation due to induce the stresses. Average grain size was $5.63378 \pm 1.55312 \mu\text{m}$. It was formed homogeneous solution and BCC structure. Iron alpha phase was formed. Grain of small size was occupied small fraction of area. Grain size of 0.25031 micron diameter was covered 0.00308813 fraction of area. Grain size of 4.16251 microns was occupied major fraction of area. Fraction of area of grain size 5.26111 micron was decreased to 0.111802. Again area fraction was increased with grain size diameter. From grains size 8.40459 micron to 21.4492 micron Area fraction was decreased linearly. Largest size grains of 21.4492 occupied very lowest area fraction. Maximum numbers of grains were orient at very low angle. Number fraction of grain 0.187566 was misorientated at angle 3.575° . 12.2787 number fraction grains boundaries are kept at 60.275° angle. High orientation angle between two grains boundaries means that it was formed more twinning boundaries

(d) Sample L

Due to addition of lanthanum oxide grain size was increased. Some grains were orientated in longitudinal direction and average grain size was $17.825 \pm 2.5877 \mu\text{m}$. Twin boundaries were formed at lower boundary angle $10-15^\circ$ and $50-60^\circ$ higher boundary angle. It was formed homogeneous solution and BCC structure. $5-60^\circ$ angle

was considered as grain boundary. From figure 5.8 (a) grains size of 0.255128 microns covered low area of fraction that was 0.00198222. With increase in diameter of grains Area fraction was expanded. After the grain size of 11.3984 microns area fraction was reduced to 0.115858. Small misorientation angle was found in large number of grains which were 0.236255 in number of fraction. Small misorientation angle was 3.575°. 0.00232821 number fraction of grains were kept at very high angle which were 60°.

From Above results of four samples have grain structure of different sizes and shape. Size of grains describe about the mechanical properties of material.

According to the Hall-Petch equation

$$f^{\circ} = f_i + K/\sqrt{D} \quad \dots(1)$$

strength of material- f°

Frictional stress- f_i

Constant factor-K

Grain size in diameter-D

This equation proved that strength of material is inversely proportional to the square root of grain size diameter. Smaller the grain size in diameter then material has more strength. These results were shown that sample N had greater strength than other samples because it's grains size was smaller than others. Lanthanum oxide was expanded the grain size than reference sample A so it had very low strength and hardness. More twin boundaries were formed in lanthanum oxide sample. It was shown that due increase in size of grains twin boundaries like defects are produced. Sample LN had also small grains due to presence of HBN. It was shown clear from above results HBN had great effect on microstructure of grain and reduce the size of grains. Increase the quantity of the HBN in composition was improved the mechanical properties of metal. Due to increase the quantity of lanthanum oxide, size of grains were expanded and reduce the strength of material.

5.2 Mechanical Properties

5.2.1 Micro hardness Test

Resistance of body to indent and ability to withstand wear is known as hardness. Hardness estimation provides microstructural modification caused by welding. Vicker

hardness test was performed under 500 grams constant for all samples. Dwell time for loading was 20 seconds. It was kept constant for each sample. Results given in following table 5.1

Table 5.1: Micro hardness value of hard-facing layers with addition of different element

Samples	Hardness (VHN)
Sample A (Reference)	241
Sample N	290
Sample L	236
Sample LN	276

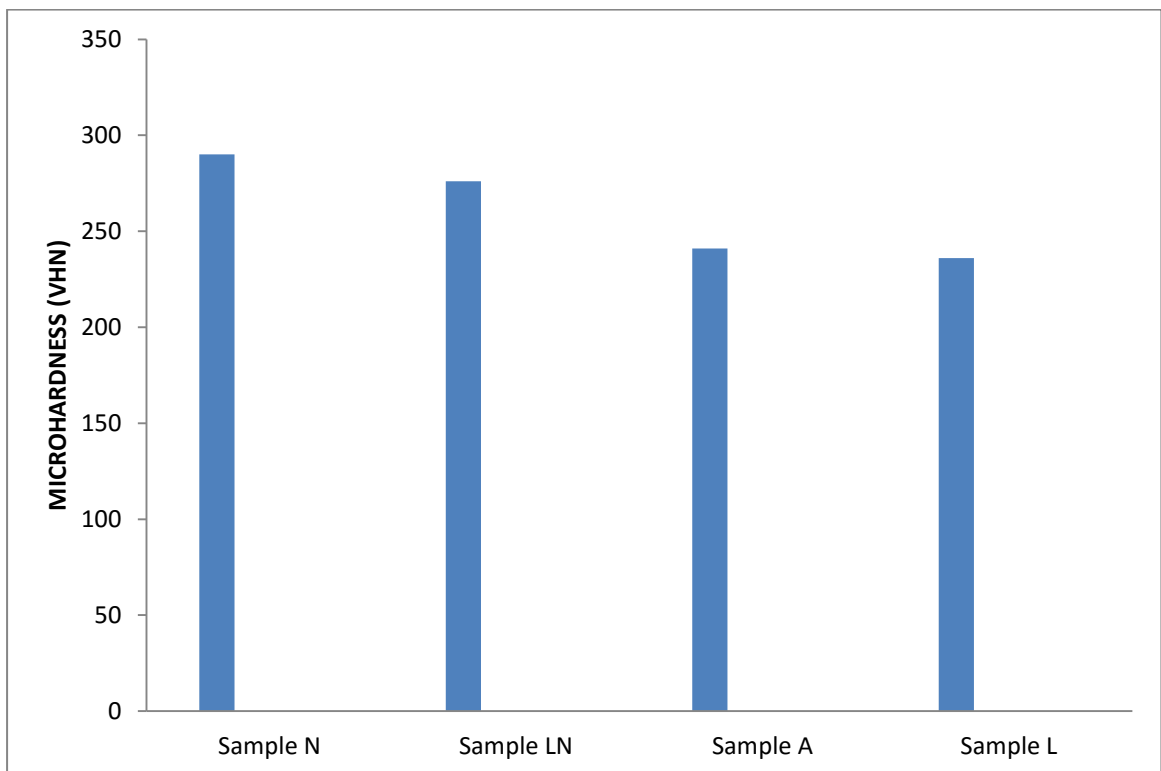


Figure 5.9 Bar graph show hardness (VHN) of hard-facing deposition of different element

Results described in Table 5.1 were average value of four readings. Figure 5.9 shows that sample with addition of HBN has hardness value of 290 VHN. Hexa boron nitride sample was increased the hardness of weld bead. HBN is hexagonal form of

boron and nitride and its chemical formula is three boron atoms and three nitrogen atoms in join with each other by strong bond whose length is 0.145 nm[22]. It has crystalline structure similar to graphite. Micro hardness of weld bead was increased uniformly by addition of hexa boron nitride. The hardness value of sample N was 20.33 % more as compared to sample A (Reference). Sample L has 236 VHN hardness value. Lanthanum oxide was shown no enhancement in hardness value of weld bead, even addition of lanthanum oxide only reduced its hardness by 2% in comparison of weld bead of sample A. 1.1 wt% content of lanthanum oxide has no influence on mechanical properties. If lanthanum oxide content is above 0.89 wt% then it has no significance on physical properties of material [16]. Sample LN in which both lanthanum and nitride addition had great influence on the physical properties of metal. It had 276 VHN hardness value. It was increased the hardness as compared to sample A but less than sample N. Combination of both rare earth oxide and hexa boron nitride was improved the surface of weld bead. With addition of HBN, hardness was increased uniformly. In sample LN, lanthanum oxide content was 0.21 wt% and HBN content was 0.21 wt%, It means La_2O_3 with content less than 0.89 wt % was improved the hardness[16]. Sample LN had 5.07% hardness less than the sample N but by 14.522% increased the hardness than sample A (Reference).

5.3 Wear test analysis

Wear is defined as relative frictional motion between two metal surfaces. It causes damage to the surface by erosion. Wear test was performed by Pin-on-disc machine. Disc of 100 mm diameter (EN31 grade steel) was used to produce relative motion with specimen. Measuring instrument of Least count error of 0.001 g was used. Weight loss was found by measuring the initial weight of sample before rotating on disc and weigh after the specimen was ran on machine. Difference between both initial weight and final weight was provided information about weight loss. Two types of loads were taken 49.05 N and 73.575 N. Single speed was selected as 2 m/s. Rpm was varied, according to the wear track diameter. Wear track diameter was changed to complete the sliding distance 600 m, 1200m, 1800 m, 2400m, 3000m, 3600m, 4200 m and so on. Wear track diameter was varied from 20 mm to 80 mm. Wear test was ran for every sample upto that sliding distance, when weight loss was became constant. Rpm was changed with respect to wear track diameter. Every sample was slide over disc for 30 minutes. Sample was travelled of 600 m sliding distance with 2 m/s speed

in 5 minutes. After the interval of 5 minutes, stop the machine and measured the weight. Weight loss was found by subtract the final weight of sample from initial weight of sample. After measured the weight loss of sample, again it was installed on the machine to complete the next sliding distance of 1200 m. Every sample was run on different track diameter of disk. Rpm was set with respect to the wear track diameter. Experiment of wear was performed on sample N, sample LN and sample A (Reference) because hardness of these samples was more as compared to sample L. This study was revealed the comparison between wear resistant of these three samples. Weld bead of all sample had same cross-section area. It was 10×3 mm². Sample was fixed in clamp and Surface of the weld bead was remained in contact with disk surface when load was applied. Weld bead was cleaned with acetone when sample was removed from the clamp and debris left on disk was cleaned when new sample was installed on machine.

5.3.1 Results of wear test was performed at 49.05 N load and 2 m/s speed

5.3.1.1 Sample A (Reference)

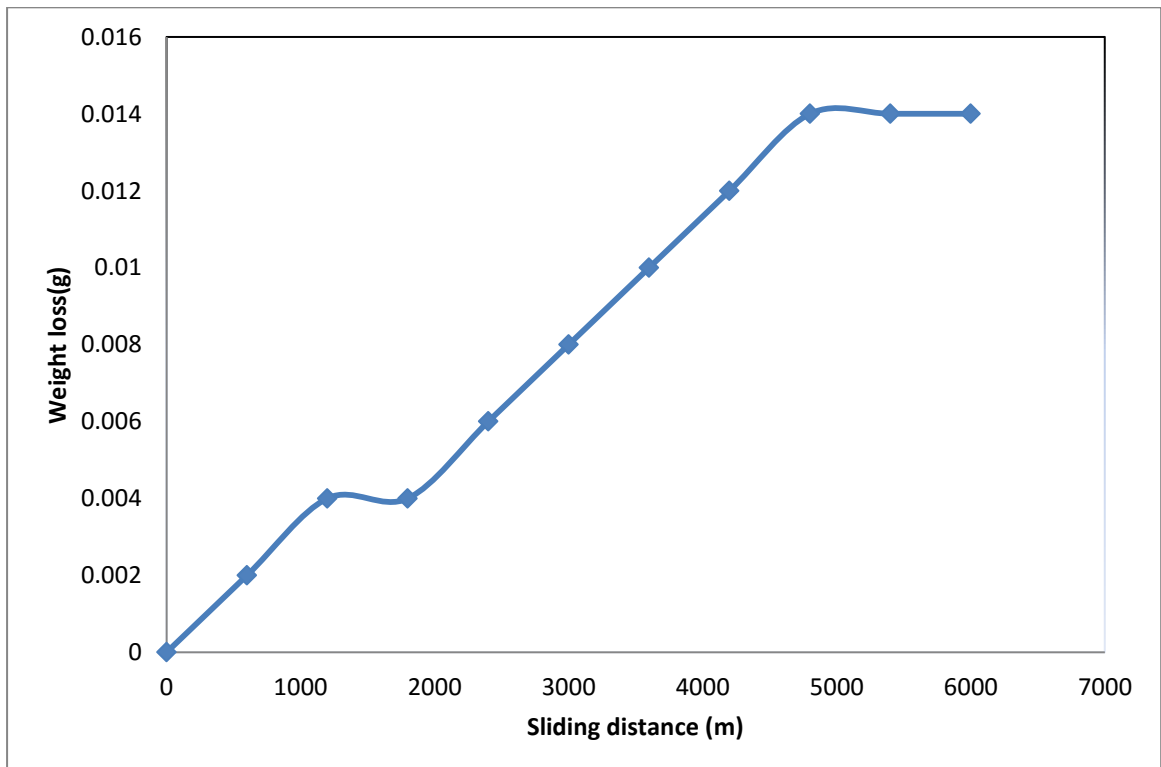


Figure 5.10 Graph plots of weight loss and sliding distance

Figure 5.10 Sample A was run on pin on disc machine. Parameters were Load 49.05 N, velocity 2m/s and 1273 RPM was set according to wear track diameter of disc.

This graph show that the trend of wear behavior of sample A. It had minimum weight loss at initial sliding distance. Sample A was slide over disc for 5 minute to cover the 600 m sliding distance at 2 m/s speed. Measured the weight loss of sample after ran for 600 m sliding distance. This Process was remained continue to that sliding distance where weight loss became constant. Minor weight loss was occurred after 4800 m sliding distance. After the sliding distance of 3000 m, slope of weight loss was raised. Maximum weight loss (Initial weight –Final weight) was 0.014 g.

5.3.1.2 Sample N

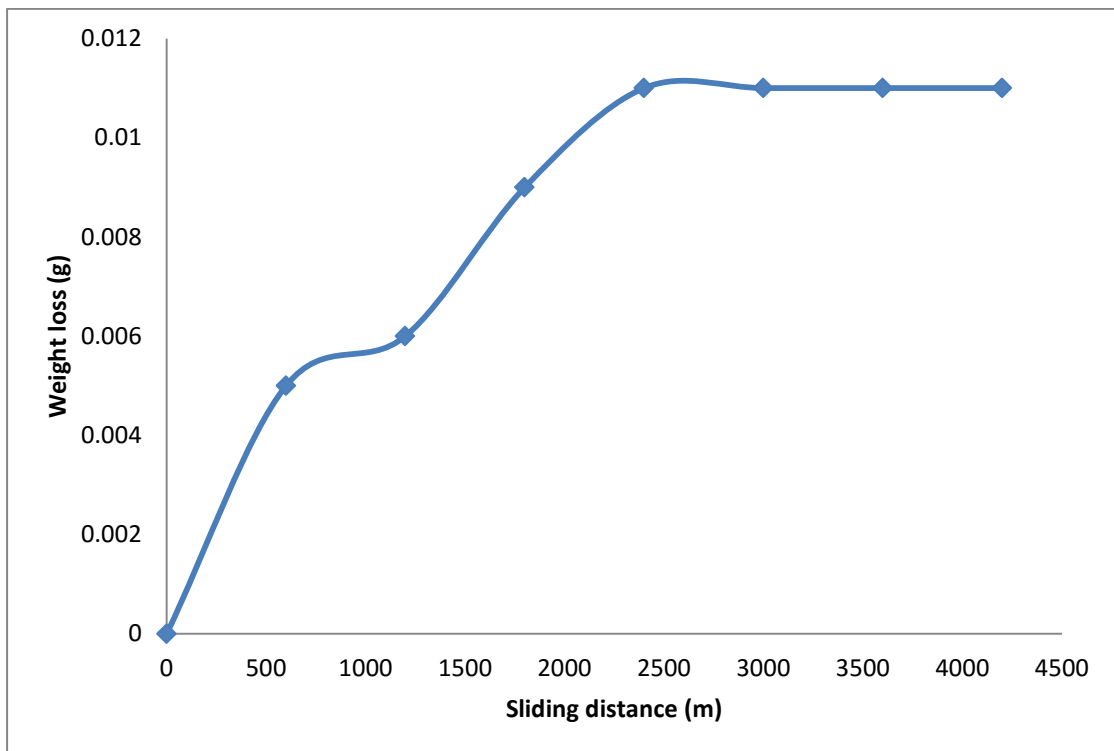


Figure 5.11 Graph plots of weight loss and sliding distance

In Figure 5.11 sample N wear test was performed on parameters load 49.05 N, velocity 2 m/s, 955 Rpm and wear track diameter was 40 mm. Slope of weight loss of sample N increased upto sliding distance 2400 m after that weight loss shown a constant trend. This trend was shown that weight loss had linear relationship with sliding distance at initial stage. It was become stagnant after travelled of 3000 m sliding distance. Maximum weight loss of sample N at sliding distance 4800 m was 0.011 g. At 600 m sliding distance weight loss was 0.005 g. At 1200 m sliding distance weight has raised to 0.006 g. After 3000 m sliding distance weight loss was stagnant.

5.3.1.3 Sample LN

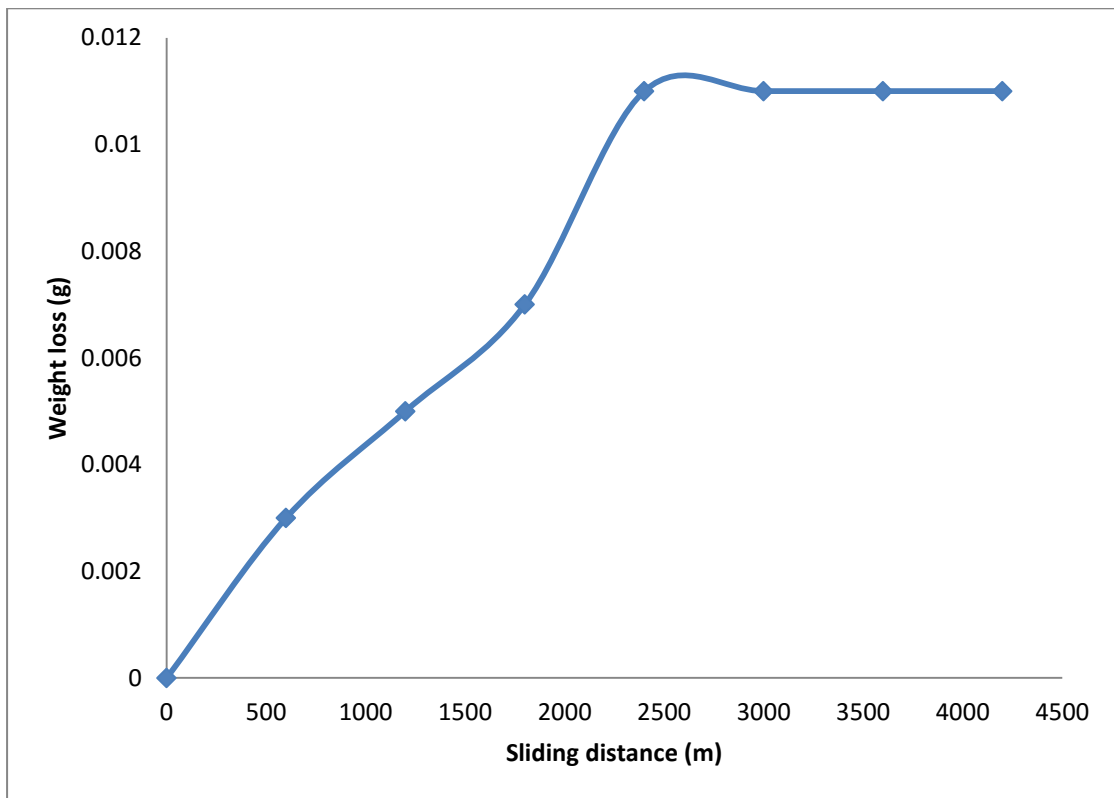


Figure 5.12 Graph plots of weight loss and sliding distance

In Figure 5.12 Sample LN performed for wear test on parameters Load 49.05 N , velocity 2 m/s 764 Rpm and wear track diameter was 50 mm. This graph shows that weight loss varied linearly sliding distance 1800 m. After that trend of graph is change it shows a more slope after sliding distance 1800 m. Weight loss increased from SD of 2400 m. After travelled 2400 m weight loss was became minimum and shows a constant trend. At 600 m sliding distance, weight loss was 0.003 g. 600 m sliding distance at speed 2m/s covered in 5 minutes. Weight the sample after every interval of 5 minutes. Weight loss at 1200 m was 0.005 g. Weight loss was became stagnant at 3000 m sliding distance. Stagnant weight loss was 0.011 g.

5.3.2 Results of wear test Performed at 73.575 N load and speed 2 m/s

5.3.2.1 Sample A (Reference)

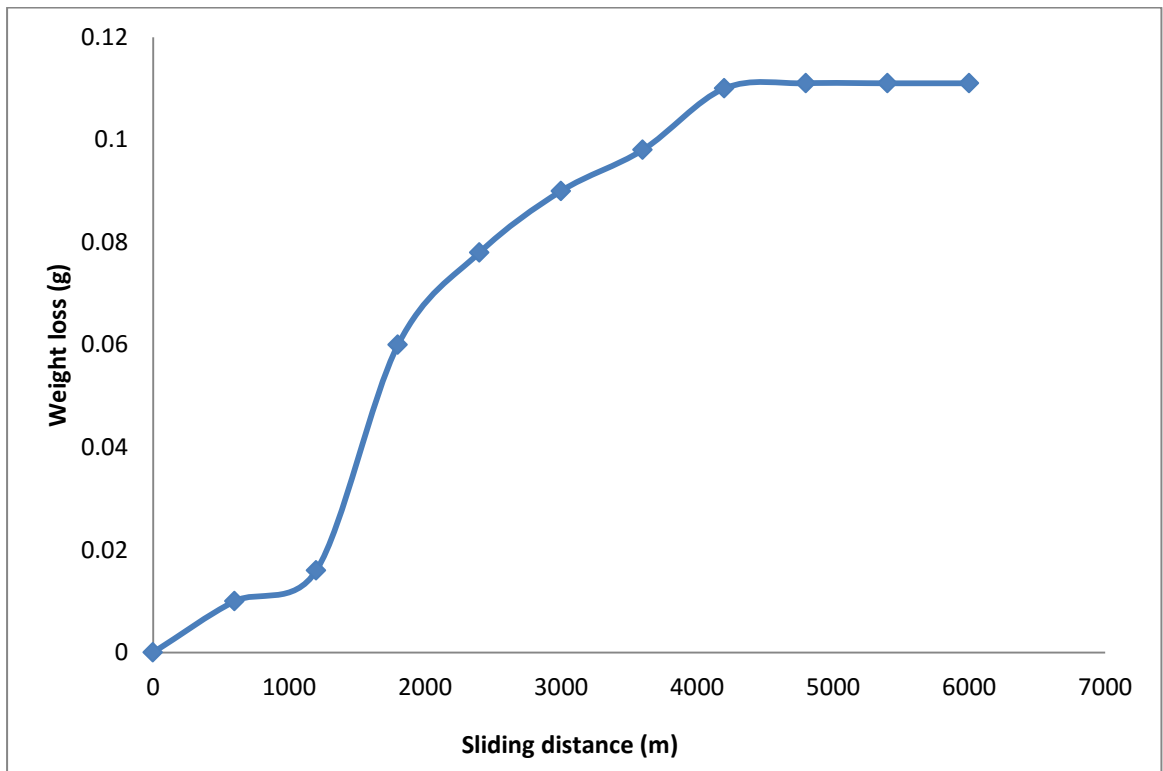


Figure 5.13 Graph plots of weight loss and sliding distance at load 73.575 N

In Figure 5.13 Sample A was ran on load 73.575 N, Speed 2 m/s, Rpm 637 and wear track diameter was 60 mm. With increase in load, weight loss was expanded. After travelled 600 m Sliding distance, it got 0.010 g weight loss and weight loss was expanded after interval of time of 5 minutes after 4200 m of Sliding distance, weight loss was diminished. It became constant and no weight loss occurred. Maximum weight loss (Initial weight – Final weight) at 6000 sliding distance was 0.111 g.

5.3.2.2 Sample N

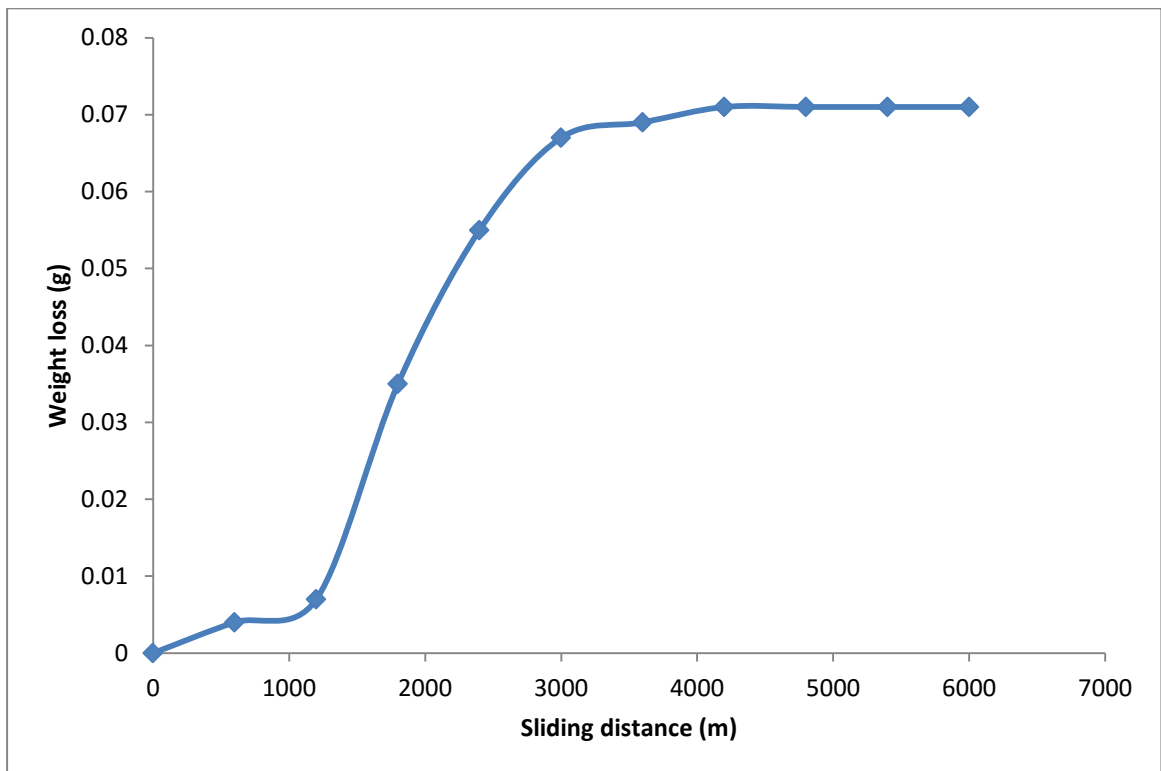


Figure 5.14 Graph plots of weight loss and sliding distance at load 73.575 N

In Figure 5.14 sample N was performed wear test on load 73.575 N, velocity 2m/s, rpm was 546 and wear track diameters was 70 mm. Trend of this graph shows that weight loss was low at starting sliding distance of 600 m after that then raised after travelled from 1200m to 3000 m. After 3600 m sliding distance graph follows constant trend. Minimum weight loss was occurred at 600 m sliding distance that was 0.004 g. Slope of weight loss was raised with Ascending of sliding distance but weight loss was become stagnant at 4800 m sliding distance.

5.3.2.3 Sample LN

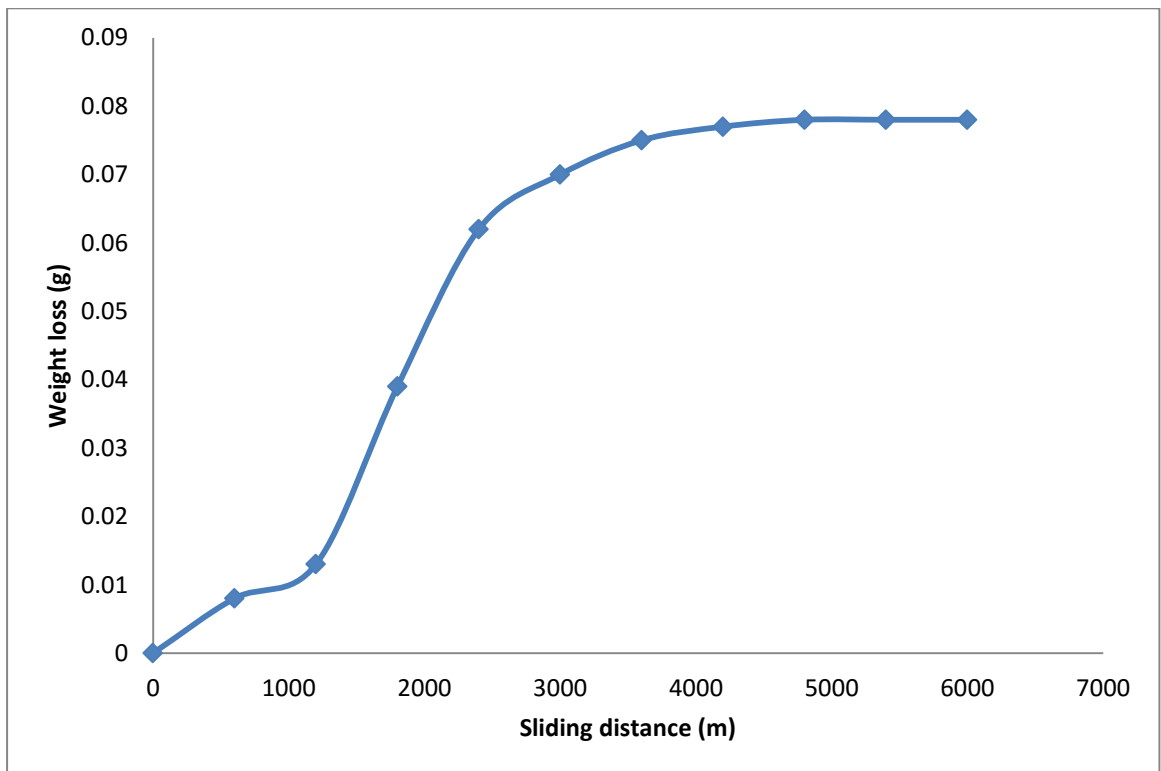


Figure 5.15 Graph plots for weight loss and sliding distance at load 73.575 N

Figure 5.15 sample LN was performed wear test on load 73.575N, velocity 2 m/s, 477 rpm and wear track diameter was 80 mm. This graph was shown same trend as sample N. At initial sliding distance weight loss was minimum at 600 m sliding distance but after ran over sliding distance of 1200 m weight loss was expanded. After 4200 m weight loss was diminished and became constant after 4800 m travelled.

DISCUSSION OF WEAR TEST

From above results it was shown very clear Weight loss was directly proportional to Load applied. There was no effect of velocity. Weight loss was increased with increase in Sliding distance but weight loss was become constant after travel some sliding distance. At starting distance weight loss and sliding distance had a linear relationship. After worn of some surface, weight loss was become constant. Hexa boron nitride had good wear resistant as compared to other. It had low weight loss and became constant after 2400 m sliding distance with minimum weight loss but with increasing load wear behavior was changed. It was become constant after 4200 m sliding distance. Sample A had poor wear resistant as compared to sample N. Hexa boron nitride had lubricating properties. It was a reason behind of great wear

resistance. Wear resistance of sample LN was better than Sample A. Sample A was got highest weight loss at both loading condition 49.05 N and 73.575 N. Effect of load was more in weight loss. It was helped to increase the weight loss. There was no significance of velocity and rpm. Weight loss of sample A at 49.05 N load was 0.002 g at initial sliding distance 600 m and maximum weight loss was 0.14 g. Weight loss was increased with increase in sliding distance. After 4800 m weight loss was became constant. At starting, slope of the weight loss was increased linearly but after 4800 m weight loss was became constant. When sample A operated at loading condition 73.575 N and speed remain constant then weight loss was maximum at initial sliding distance that was 0.10 g but here load was significant factor due to high load weight loss was increased with sliding distance. Again weight loss became constant after 4800 m and highest weight loss at 73.575 N was 0.111 g. For sample N weight loss at 49.05 N load was 0.005 g at initial sliding distance 600 m. Weight loss in sample N became constant after 2400 m sliding distance and maximum weight loss in sample N at 49.05 N load was 0.011 g and remained constant from 2400 m to 6000 m sliding distance. Sample N at load 73.575 N had weight loss was 0.004 g which was lower than sample A weight loss at same condition. Material loss became constant after 4200 m sliding distance. Maximum weight loss at 73.575 N load was 0.071 g which was very low as compared to sample A. Now, If we talk about sample LN that it was shown also minimum weight loss than sample A but more than sample N. Weight loss of sample LN at load 49.05 N was 0.003 g at 600 m sliding distance. Weight loss became constant after 2400 m sliding distance. Constant weight loss of sample LN was 0.011 g. When loading condition was changed from 49.05 N to 73.575 N weight loss was increased. At this condition weight loss was 0.008 g upto sliding distance 600m. Weight loss became constant after 4800 m. Constant weight loss was 0.078 g which was higher than Sample N and lower than sample A. It means combination of lanthanum and HBN was good composition to improved the tribological properties of substrate. It was proved that HBN had a great influence on the wear resistance. If content of HBN was raised then physical properties of material was improved.

5.3.3 SEM Images of wear samples

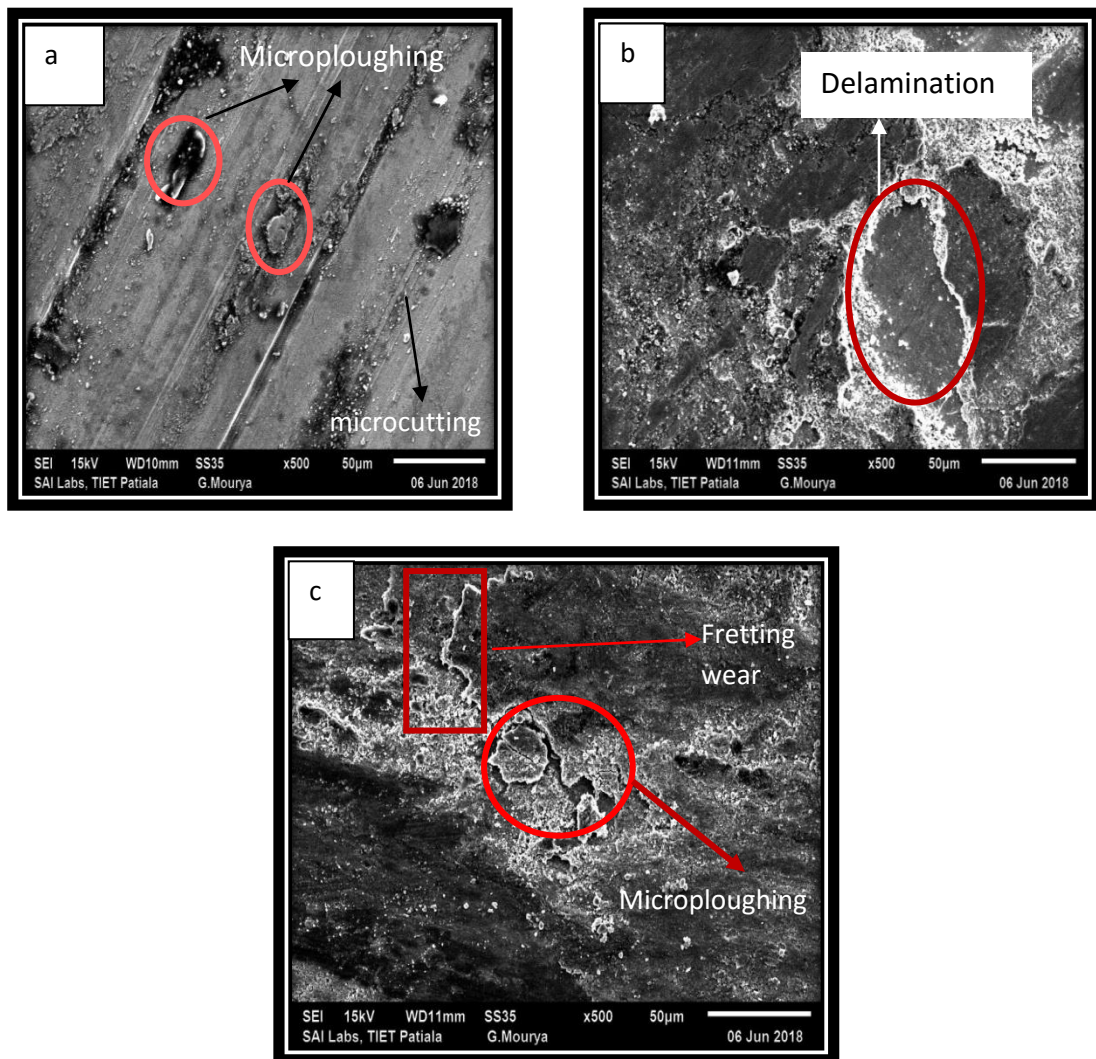


Figure 5.16 SEM images of surface of weld bead of wear sample (a) Sample N (b) Sample A (c) Sample LN

Figure 5.16 (a) shows that some chips were formed due to micro cutting. Surface of weld bead of sample N was hard there was no pitting or spallation had shown. Micro-ploughing and micro cutting was observed. Micro-ploughing was shifted of material but not removed from the surface. Micro-cutting was volume removed equal to the wear track.

Figure 5.16 (b) shows surface morphology of wear mechanism of Sample A. Delamination was occurred over the surface of weld bead. Reason behind the delamination was plastic deformation of the surface. Continuous removal of material from the surface of weld bead was delamination. Due to cyclic load or fatigue of surface, loss of material raised.

Figure 5.16 (c) shows fretting wear was occurred over the surface of weld bead of sample LN. Fretting wear was occurred due to cyclic sliding of the two metal surface. Micro ploughing was observed also. Holes and cavities show that material was removed from the surface.

5.4 Results for corrosion test of weld bead

This experiment was performed in salt spray chamber. It provides information about relative corrosion resistance. Weld bead was exposed to corrosive environment. Salt solution of 3.5% Nacl concentration was sprayed over the weld bead. It was accelerate the corrosion of weld bead. Samples were placed in salt spray chamber for 120 hours. Parameter was remained constant like temperature was $29\pm 2^{\circ}$ C and relative humidity was $95\pm 2\%$.

5.4.1 Sample A (Neutral)

Table 5.2

Time	Corrosion percentage (results)
At 0 hours	No sign of white or yellow spots
At 24 hours	No sign of white or yellow spots
At 48 hours	No sign of white or yellow spots
At 72 hours	No sign of white or yellow spots
At 96 hours	8 to 10% white +yellow spots
At 120 hours	35 to 40% white + yellow spots

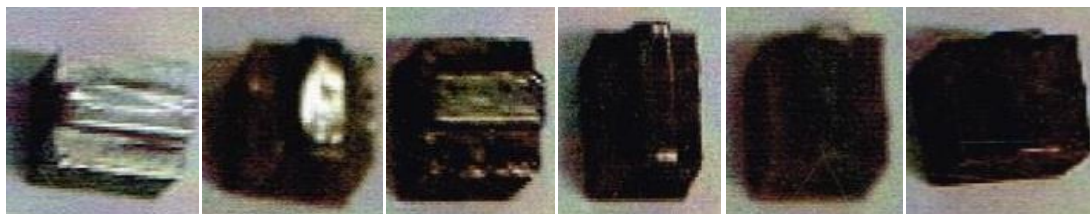


Figure 5.17 Corrosion of weld bead of sample A from 0 hours to 120 hours

5.4.2 Sample N (HBN)

Table 5.3

Time	Corrosion percentage (results)
At 0 hours	No sign of white or yellow spots
At 24 hours	No sign of white or yellow spots
At 48 hours	No sign of white or yellow spots
At 72 hours	No sign of white or yellow spots
At 96 hours	10 to 15% white + yellow spots
At 120 hours	50 to 60% white +yellow spots

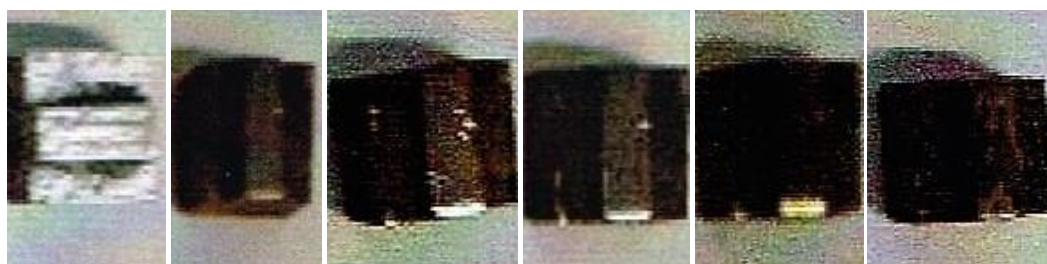


Figure 5.18 Corrosion of weld of sample N from 0 hour to 120 hours

5.4.3 Sample L (Lanthanum oxide)

Table 5.4

Time	Corrosion percentage (results)
At 0 hours	No sign of white or yellow spots
At 24 hours	No sign of white or yellow spots
At 48 hours	No sign of white or yellow spots
At 72 hours	No sign of white or yellow spots
At 96 hours	0 to 5% white + yellow spots
At 120 hours	10 to 15% white + yellow spots

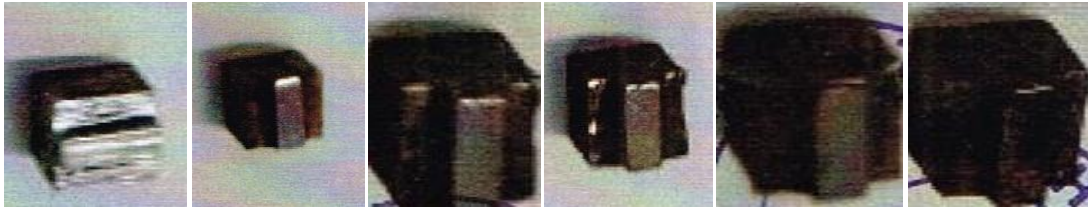


Figure 5.19 Corrosion of weld bead of sample L form 0 hour to 120 hours

5.4.4 Sample LN (Lanthanum and HBN)

Table 5.5

Time	Corrosion percentage (results)
At 0 hours	No sign of white or yellow spots
At 24 hours	No sign of white or yellow spots
At 48 hours	No sign of white or yellow spots
At 72 hours	No sign of white or yellow spots
At 96 hours	0 to 5% white + yellow spots
At 120 hours	10 to 15% white + yellow spots

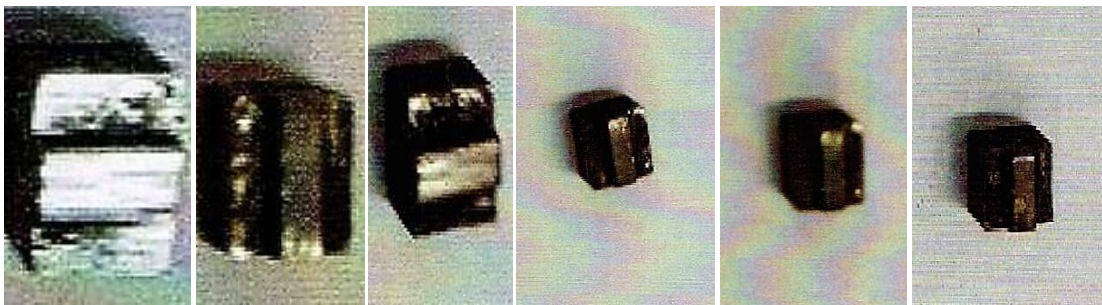


Figure 5.20 Corrosion of weld bead of sample LN from 0 hour to 120 hours

Due to constant parameter of corrosion test like Relative humidity $95\pm 2\%$ and Ambient temperature 29 ± 2 °C Corrosion was varying with increasing time.

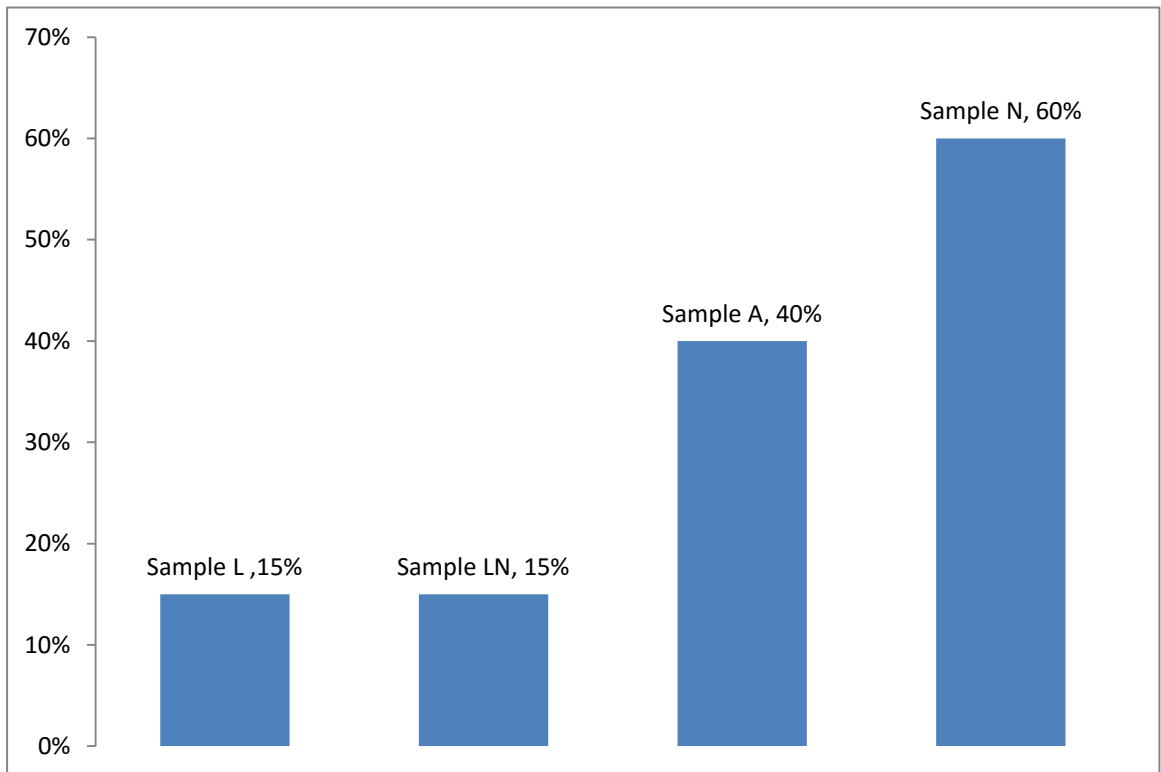
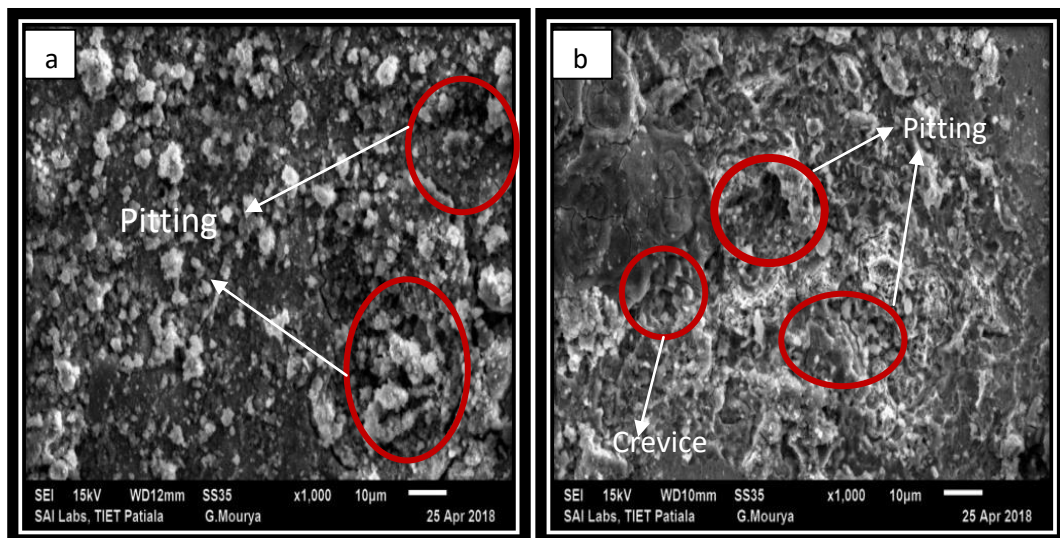


Figure 5.21 Corrosion %age of area of weld bead of each sample

5.4.5 SEM Images of corrosion samples



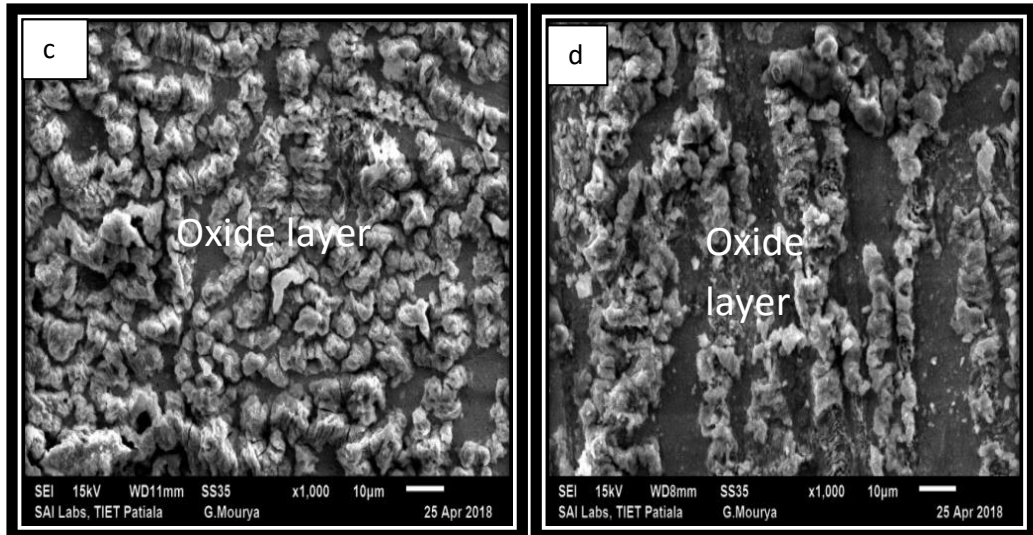


Figure 5.22 SEM images of surface morphology of corrode weld bead (a) Sample A (b) Sample N (c) Sample L (d) Sample LN

5.4.6 Sample N

It observes from Figure 5.21 data that hexa boron nitride was increased the corrosion rate as compare to other samples. The 60% area of weld bead got corroded when kept in salt spray chamber for 120 hours. It was reduced the corrosion resistant. Sample A in which no alloys was added had good corrosion resistant as compared to sample N. In sample A, 35 to 40% Area of weld bead got corrosion. Lanthanum oxide (Rare earth oxide) was showed a great improvement in corrosion resistant. 10 to 15% area of weld bead got corroded after 120 hours. From figure 5.22 (b) it was observed that sample N got pitting corrosion and crevice corrosion which helps in development of cavities and holes. Weight loss occurred due to holes and cavities was formed on surface of weld bead of sample N. Surface of the weld bead of sample N got deteriorate and no formation of oxide layer was formed.

5.4.7 Sample L

It was showed the good corrosion resistance. There was no any formation of pitting or crevice like corrosion. Oxide layer was formed on the surface of weld bead. It was protected the surface of weld bead from deterioration. Oxidation reaction was not placed over surface of weld bead. With Increase the content of lanthanum oxide, corrosion resistant was increased uniformly. Figure 5.22 (c) shows that lanthanum oxide was formed a protective layer on the surface of weld bead which was prevented it from corrosion. Lanthanum is acting on the surface of weld bead. Lanthanum oxide

was formed a oxide layer on the surface of weld bead, which was uniform in nature. This layer was resisted the surrounding impurities to diffuse in the interior of alloys. Lanthanum had low electro-negativity (tendency to gain electron) which diminished the number of oxygen and sulfur (these are both corrosion accelerator) [14]. It prevented the surface from pitting corrosion. Any type of hole or cavities was not found in sample L. Material loss was negligible for 120 hours of working process of salt spray chamber for sample L.

5.4.8 Sample LN

Sample LN was shown a good corrosion resistance as compared to sample N and sample A. Combination of both lanthanum oxide and HBN had good performance in improvement of physical properties as well as chemical properties. It got 10 to 15 % area of weld bead corroded. It was shown same results like sample L. Content of lanthanum oxide in composition of alloys was prevented the surface of weld bead from corrosion. Corrosion resistance was uniform in sample LN and sample L. There was no significance of variation in wt% of lanthanum oxide. From figure 5.22 (d) It was observed that there was formation of layer of oxide which was protected the surface of weld bead from surrounding impurities. HBN was not acted as corrosion accelerator in sample LN. Lanthanum oxide was reduced the effect of hexa boron nitride.

CHAPTER 6

CONCLUSIONS

The conclusions from present research work were drawn regarding the behavior of hexa boron nitride and lanthanum oxide subjected to hard-facing technique. Hard-facing effects on microstructure evolution with change in size of grains have been reported. Hard-facing was done by manual arc welding. Wear test was performed in this analysis to find the good wear resistance. The effect of grains size on the strength of weld bead was discussed. Corrosion behavior of weld bead with addition of different weld bead was studied. The conclusions from present study are elaborated below:

- As hexa boron nitride was increased in quantity then hardness of the weld bead was also increased than sample A (Reference). It was improved the mechanical properties of weld bead.
- HBN reduced the grain size in diameter. According to Hall-Petch equation it was found that if grain size has small diameter in μm then it has more strength because strength is inversely proportional to square root of diameter of grain. EBSD test was shown that HBN refined the microstructure and reduced the size of grains. Micro hardness test was proved that HBN had more hardness because of small grains than others samples. Less twin boundaries were found in HBN sample.
- HBN reduced the corrosion resistance. Although it was improve the mechanical properties but rate of corrosion increased. It was shown pitting and crevice corrosion. No oxide layer was formed over the surface of weld bead.
- HBN was shown great wear resistance as compared to others. Weight loss was become constant after short distance travelled. Wear resistance performance was best because of its high hardness and small grain size.
- Lanthanum oxide (La_2O_3) was shown no improvement in hardness. It reduced the hardness than Reference Sample A.
- Lanthanum had grain size large in diameter. That was why it had poor mechanical properties.

- Lanthanum was shown good corrosion resistance. It was formed oxide layer over the surface of weld bead. It was protected the surface of weld bead from oxidation reaction. No pitting or weight loss occurred in this sample
- Combination of lanthanum oxide and HBN was improved the hardness as compared to reference sample A but less than hexa boron nitride (Sample N). Mixture of both alloys was improved the surface of weld bead. HBN was improved the Wear resistance and hardness and Lanthanum oxide was improved the corrosion resistance. Mixture of both elements had grains, smaller in size but larger than HBN that was why it had hardness less than sample N. Lanthanum oxide was shown its own effect in combination of both elements, it was reduced the corrosion and improved the corrosion resistance.

REFERENCES

- [1] Buchely, M.F., Gutierrez, J.C., Leon, L.M. and Toro, A., 2005. The effect of microstructure on abrasive wear of hard-facing alloys. *Wear*, 259(1-6), pp.52-61.
- [2] Buchanan, V.E., Shipway, P.H. and McCartney, D.G., 2007. Microstructure and abrasive wear behaviour of shielded metal arc welding hard-facings used in the sugarcane industry. *Wear*, 263(1-6), pp.99-110.
- [3] Wang, J., Liu, T., Zhou, Y., Xing, X., Liu, S., Yang, Y. and Yang, Q., 2017. Effect of nitrogen alloying on the microstructure and abrasive impact wear resistance of Fe-Cr-C-Ti-Nb hardfacing alloy. *Surface and Coatings Technology*, 309, pp.1072-1080.
- [4] Gou, J., Wang, Y., Sun, J. and Li, X., 2017. Bending strength and wear behavior of Fe-Cr-CB hardfacing alloys with and without rare earth oxide nanoparticles. *Surface and Coatings Technology*, 311, pp.113-126.
- [5] Wang, H. and Yu, S., 2017. Influence of heat treatment on microstructure and sliding wear resistance of high chromium cast iron electrosag hardfacing layer. *Surface and Coatings Technology*, 319, pp.182-190.
- [6] Sadeghi, F., Najafi, H. and Abbasi, A., 2017. The effect of Ta substitution for Nb on the microstructure and wear resistance of an Fe-Cr-C hardfacing alloy. *Surface and Coatings Technology*, 324, pp.85-91.
- [7] Ding, Y., Liu, R., Yao, J., Zhang, Q. and Wang, L., 2017. Stellite alloy mixture hardfacing via laser cladding for control valve seat sealing surfaces. *Surface and Coatings Technology*, 329, pp.97-108.
- [8] Ripoll, M.R., Ojala, N., Katsich, C., Totolin, V., Tomastik, C. and Hradil, K., 2016. The role of niobium in improving toughness and corrosion resistance of high speed steel laser hardfacings. *Materials & Design*, 99, pp.509-520
- [9] Molleda, F., Mora, J., Molleda, F.J., Carrillo, E., Mora, E. and Mellor, B.G., 2006. Mild steels coated with 14% manganese covered electrodes (E7-UM-

200-K and E1-UM-350): Phenomena at the steel-coating interface. *Materials characterization*, 57(4-5), pp.300-305.

- [10] Wang, J.B., Zhou, Y.F., Xing, X.L., Liu, S., Zhao, C.C., Yang, Y.L. and Yang, Q.X., 2016. The effect of nitrogen alloying to the microstructure and mechanical properties of martensitic stainless steel hardfacing. *Surface and Coatings Technology*, 294, pp.115-121.
- [11] Hejwowski, T., 2006. Investigations of corrosion resistance of Fe-, Ni- and Co-based hardfacings. *Vacuum*, 80(11-12), pp.1386-1390.
- [12] Singla, Y.K., Arora, N., Dwivedi, D.K. and Rohilla, V., 2017. Influence of niobium on the microstructure and wear resistance of iron-based hardfacings produced by pre-placement technique—a novel approach. *The International Journal of Advanced Manufacturing Technology*, 93(5-8), pp.2667-2674.
- [13] Singla, Y.K., Arora, N. and Dwivedi, D.K., 2017. Dry sliding adhesive wear characteristics of Fe-based hardfacing alloys with different CeO₂ additives—A statistical analysis. *Tribology International*, 105, pp.229-240.
- [14] Dong, Y., Jianshe, C., Qing, H. and Kuiren, L., 2009. Effects of lanthanum addition on corrosion resistance of hot-dipped galvalume coating. *Journal of rare earths*, 27(1), pp.114-118.
- [15] Cajner, F., Kovačić, S., Rafael, H., Vugrinčić, A., Šimunović, V. and Gržeta, B., 2015. Influence of nitriding on corrosion resistance of martensitic X17CrNi16-2 stainless steel 46(1), pp.69-77.
- [16] Yan, C., CHENG, M., Hongwu, S.O.N.G., ZHANG, S., Jinsong, L.I.U. and Yan, Z.H.U., 2014. Effects of lanthanum addition on microstructure and mechanical properties of as-cast pure copper. *Journal of Rare Earths*, 32(11), pp.1056-1063.
- [17] Singla, Y.K., Dwivedi, D.K. and Arora, N., 2015. On the modeling of dry sliding adhesive wear parameters of vanadium additive iron-based alloys at elevated temperatures. *Surface and Coatings Technology*, 283, pp.223-233.

- [18] Singla, Y.K., Chhibber, R., Arora, N., Singh, K. and Khanna, K., 2017. On the Microstructure and Wear Behavior of Fe-xCr-4Mn-3C Hardfacing Alloys. *Transactions of the Indian Institute of Metals*, 70(6), pp.1555-1561.
- [19] <http://shodhganga.inflibnet.ac.in/bitstr>
- [20] <https://www.weldingalloys.com/uploads/pdf/brochures/en/waconsumables/fundamentals-of-hardfacing-arc-welding.pdf>
- [21] <https://www.wikipedia.org>
- [22] <http://www.docbrown.info/page03/nanochem06.htm>